Fermi National Accelerator Laboratory

FERMILAB-Pub-78/14-THY
January 1978

A Comparison of Trimuon Production Mechanisms

C. H. Albright*

Fermi National Accelerator Laboratory
Batavia, Illinois 60510

J. Smith

Institute for Theoretical Physics, State University of New York at Stony Brook
Stony Brook, New York 11794

and

J. A. M. Vermaseren

Department of Physics, Purdue University
West Lafayette, Indiana 47907

ABSTRACT

We compare the predictions of six models for neutrino (and antineutrino) production of trimuon events. In particular, results are given for models based on heavy charged lepton decays, heavy neutral lepton decays together with heavy quark decays, diffractive production and decay of heavy quark pairs, heavy quark cascade decays, the decays of Higgs mesons, and the radiative production of muon pairs. Our comparison should help to unravel the sources of the trimuon events detected at Fermilab and CERN. We also examine the probability of explaining the so-called super-events where the muons are extremely energetic.

*Permanent address, Department of Physics, Northern Illinois University, De Kalb, Illinois 60115.

Operated by Universities Research Association Inc. under contract with the Energy Research and Development Administration

I. INTRODUCTION

In the past year, observation of events with three muons in the final state has been reported by several experimental groups, using both narrow- and wide-band neutrino and antineutrino beams. In particular, by summer 1977 two events were found by the Caltech-Fermilab (CF) group,[1] thirteen events were recorded by the Fermilab-Harvard-Pennsylvania-Rutgers-Wisconsin (FHPRW) collaboration[2] and three were detected by the CERN-Dortmund-Heidelberg-Saclay (CDHS) group.[3] At the time of this writing, all three experimental groups are continuing to take more data and have reportedly accumulated many more trimuon events, as well as two tetramuon events.[4]

While some of these events probably arise from prompt pion and kaon decay backgrounds, at least two "super" events have been found[2] which most certainly do not arise from this mechanism. For these events, the observed muon energies are large: (157, 32 and 47 GeV) and (96, 73 and 83 GeV); while the observed hadron energies are small (E_{had}=13 GeV) and ($E_{had} \lesssim 30$ GeV) respectively.

Numerous models have been proposed in the literature to explain the trimuon events: heavy lepton cascade decay;[5,6] simultaneous heavy lepton and heavy quark decays;[7,8] heavy quark pair production and decay;[9,10] heavy quark cascade decay;[11] Higgs production and decay;[12] and finally production of a muon pair by radiation off the muon and quark lines.[13,14] Unfortunately it is difficult to compare the model predictions directly, since the authors involved have not always made the same detailed tests for these models. In this paper we report on a systematic study of all these models and present some of the most critical tests for the viability of each model.

We have tried to make this paper rather brief and avoided any discussion of incorporating the heavy leptons and heavy quarks into gauge theory models. Many papers already exist on this subject.[15] Since the rates for trimuon production are still unclear, it is more profitable to discuss characteristic distributions for each of the classes mentioned above. We therefore only give a short summary of the models in Section II, leaving out details which can be found in published papers. However, in two cases, namely the heavy quark pair production and decay and the heavy quark cascade decay, our models differ from those discussed previously, so some additional information is given.

The results presented in Section III are flux averaged with the quadrupole triplet wide-band spectrum used by the FHPRW group. We have examined the effects of using a narrow-band spectrum but do not find that this changes our conclusions. There are many correlations which can be measured in the trimuon events, so it should be rather easy to distinguish between classes of models once a sufficient number of events is measured. Note that it is always possible to make slight changes in the predictions of each model by varying the parameters but there are significant differences between the classes of models. In the event that several sources are responsible for the trimuon events, then the comparison with theoretical models will be more difficult.

In Section IV we give a short summary of our results. Also, we make some comments on the relative sizes of event rates for dimuon, trimuon and tetramuon production in neutrino and antineutrino beams. In particular the presence or absence of a $\mu^-\mu^-$ signal in neutrino interactions is extremely important in furthering our understanding of the physics behind trimuon phenomena. Bubble chamber data on multilepton events containing electrons and/or positrons will also be very useful. Model-dependent limits on the masses of charged heavy leptons have already been presented by the B.N.L.-Columbia collaboration.[16]

II. PROPOSED MODELS

We sketch here briefly the models of interest to us which we wish to compare. Further details can be found in the listed references. In general, the models can be divided into two classes, namely those models which involve new quarks or leptons, and those that do not. In the latter category one can envisage the production of muon pairs (from trivial or non-trivial sources) in regular neutrino events. For instance the radiative production of muon pairs or the production and decay of vector mesons will yield trimuon events. If these types of mechanisms are responsible for the trimuon events seen by the FHPRW and CDHS groups, then one does not expect to see any genuine same-sign dimuon signal, so the $\mu^-\mu^-$ event rate will be due to misidentified trimuons and be much smaller than the $\mu^-\mu^-\mu^+$ event rate. The production of a Higgs scalar meson followed by its decay $H \to \mu^+\mu^-$ is another example (albeit academic) of this type.

The class of models which explain the trimuon events by invoking the production and decay of new heavy leptons and/or new heavy quarks has the feature that the multilepton event rates are controlled by the branching ratios for the heavy lepton and/or heavy quark decays. Assuming that the semi-leptonic decays of these new leptons or hadrons (which contain the new quarks) are suppressed compared to their hadronic decays, we expect to find a pattern in the multi-lepton decay rates. The $\mu^-\mu^-$ rate should be larger than the $\mu^-\mu^-\mu^+$, which in turn is larger than the $\mu^-\mu^-\mu^+\mu^+$, etc. This pattern is still expected to hold, even when events containing electrons and positrons are included and misidentified as muonic events. We also already know that there is no strong $\mu^-\mu^+\mu^+$ signal which imposes restrictions on the kind of decay chains allowed. Hence the identification of a large $\mu^-\mu^-$ or μ^-e^- event rate is necessary for establishing the validity of these models. Note that we exclude any discussion of opposite sign dimuon pairs because they will be hard to observe in the presence of single charm production and decay. An analysis of $\mu^-\mu^+$ signals will be reported later.

The models we consider fall into both classes. The first two only allow the production of muon pairs, while the other four are representative of different types of heavy hadron or heavy lepton models. The multimuon event rates for the latter four models are uncertain until specific gauge theories are constructed. However, the experimental rate is also uncertain and that is why we concentrate on distributions to distinguish one model from another.

A. Dalitz Production of Muon Pairs.

In this model, a virtual photon is radiated from the charged muon and quark lines, and converts into a real muon pair; i.e.,

$$\nu_\mu + N \to \mu^- + \text{"}\gamma\text{"} + X \quad \text{"}\gamma\text{"} \to \mu^+\mu^- \quad . \tag{2.1}$$

To maintain gauge invariance in the calculation, all the diagrams shown in Fig. 1 must be considered. In addition, the two identical muons should be antisymmetrized. Two of the authors (J.S. and J.V.) have reported results for this model in a recent paper,[13] to which we refer the reader for details. We discuss some of the important results in Section III. Note that the electromagnetic production of real vector mesons ρ, ψ, Υ etc., has been discussed by Godbole[12] and her conclusion is that the rate is too small to account for the experimental value for trimuon production.

If this radiative mechanism is the only one contributing to trimuon production, then we do not expect to see genuine dimuons or tetramuons. Hence $\mu^-\mu^-$ events will only occur if the μ^+ does not survive the energy cut and its rate will be approximately one order of magnitude smaller than the trimuon production rate. The $\mu^-\mu^+$ mode will occur at the same level as the $\mu^-\mu^-$, but will be buried in the opposite sign dimuon signal from the decays of charmed particles. Tetramuon events must arise from some background process such as π or K decay in flight. Events containing $\mu^-e^-e^+$ particles will be seen in bubble chamber exposures with an e^-e^+ invariant mass larger than that of the π^0. However, μ^-e^- events will be extremely rare.

B. Higgs Boson Production and Decay.

In this process, a scalar Higgs particle can be emitted from the muon, quark or intermediate vector boson lines. Since the effective coupling is proportional to the mass of the field which emits the Higgs particle, the emission from the W boson line is by far the most important. This diagram is illustrated in Fig.2. Godbole[12] has investigated this mechanism for Higgs boson masses in the range 3 to 7 GeV/c^2. We only consider the decay mode of the Higgs particle into a dimuon pair. Hadronic decays involving charmed particles will also lead to events with a $\mu^+\mu^-$ pair, but the invariant mass of the pair will not peak at a fixed value. Hence we consider the reaction

$$\nu_\mu + N \rightarrow \mu^- + H + X, \quad H \rightarrow \mu^+\mu^- \qquad (2.2)$$

where H stands for the Higgs particle, whose mass we take to be 4 GeV/c^2.

Our motivation for including this particular mechanism is to understand its kinematic features. We are well aware that the two-body branching ratio for $H \rightarrow \mu^+\mu^-$ will be extremely small and therefore B will be much too small to account for the trimuon event rate. However, reaction (2.2) is an example of the production of a dimuon pair with large invariant mass as compared to model A, which involves the production of a dimuon pair with small invariant mass. If reaction (2.2) is to be the explanation of the trimuon events, then we would expect a much lower rate for $\mu^-\mu^-$ events and no genuine tetramuon events. Bubble chamber experiments would never see $\mu^-e^-e^+$ events because the branching ratio for $H \rightarrow e^+e^-$ is proportional to the lepton mass and therefore exceedingly small.

C. Hadron (Quark) Cascade.

In this model one assumes that a charge 2/3 t quark is excited in neutrino interactions, which subsequently decays into lighter mass quarks. Soni[11] has considered both the quark chain $t \to b \to u$ and the chain $t \to b \to \tau$ where τ is the heavy lepton discovered by Perl et al.[17] Barnett and Chang[7] have investigated the decay $t \to \mu^+ + M^o + X$ where M^o is a neutral heavy lepton which decays into $\mu^- + X$. We investigate the decay chain

$$
\begin{array}{l}
\nu_\mu + N \to \mu^- + T + X \\
\qquad\qquad\quad \hookrightarrow B + X' \\
\qquad\qquad\qquad\quad \hookrightarrow C + \mu^- + \bar{\nu}_\mu \\
\qquad\qquad\qquad\qquad\quad \hookrightarrow S + \nu_\mu + \mu^+
\end{array}
\qquad (2.3)
$$

as illustrated in Fig. 3, where T, B, C and S refer to hadrons containing a top, bottom, charm or strange quark and X, X' represent any other hadrons. The μ^+ could instead be emitted in the T-B transition, but there are no experimental indications of a strong $\mu^-\mu^+\mu^+$ signal so we have to assume that the semileptonic decay width of $T \to B$ is suppressed compared to its non-leptonic decay width. As we expect the more massive quarks to have many hadronic decay channels, the assumption is not unreasonable.

This model allows the emission of zero to four leptons with increasing powers of the leptonic branching ratio which emphasizes the importance of knowing the event rates for multilepton signals. In the absence of detailed information on these rates, we choose the chain in (2.3) for the purpose of illustrating the typical distributions expected from a hadronic decay chain. The quark transition $d \to t$ involved in the production process is assumed to be right-handed as are the $t \to b$ and $b \to c$ transitions. We take the quark masses m_t, m_b, m_c and m_s equal to 7.5, 4.75, 1.5 and 0.5 GeV/c^2, respectively.

D. Diffractive Production of Heavy Quark Pairs.

Bletzacker and Nieh[9] have considered associated production of charm at small x as the mechanism responsible for trimuon production. From charge conservation it is clear that $c\bar{c}$ pairs cannot be produced in a normal diffractive way (via Pomeron exchange) from a charged W boson. Production of $c\bar{c}$ pairs at intermediate x has been discussed by Goldberg[10] in the framework of QCD. We consider here the diffractive production of a $c\bar{b}$ pair from a W^+ boson and assume that a gluon is exchanged between one of the quarks and the hadron vertex. This is shown in Fig. 4 for the reaction

$$\begin{array}{l} \nu_\mu + N \to \mu^- + C + \bar{B} + X \\ \quad C \to S + \nu_\mu + \mu^+ \\ \quad \bar{B} \to \bar{C} + X' \\ \qquad \bar{C} \to \bar{S} + \mu^- + \bar{\nu}_\mu \end{array} \tag{2.4}$$

Alternatively, a μ^+ could be emitted in the $\bar{b} - \bar{c}$ transition, but this would imply that many $\mu^-\mu^+\mu^+$ events would be observed as well as $\mu^-\mu^-\mu^+$ events which does not appear to be the case. In principle, four muons can arise from this diffractive process, and the event rates are proportional to the product of the semileptonic decay rates. The choice of a nonleptonic $\bar{b} \to \bar{c}$ transition is in agreement with the choice in the previous model. We have used the same values for the quark masses as given above.

Thus our model is very similar in spirit, and in computational details, to the Bletzacker-Nieh model. We assume the production cross section to be determined by a structure function F(x,y) given by

$$F(x,y) = \frac{Q^2}{(Q^2+4M_o^2)} \left(\frac{s-s_o}{s}\right)^3 e^{-10z'} \left[1 + (1-y)^2\right] ,$$

where $x = Q^2/(2M\nu)$, $y = \nu/E$, $s = 2M\nu - Q^2 + M^2$ and M is the nucleon mass. The threshold factor s_o, mass M_o and z' variable depend on the masses of the quarks. We have chosen $M_o = M_B - M$, $s_o = [M + (m_c + m_b)]^2$, and $z' = [Q^2 + (m_c + m_b)^2]/(2M\nu)$, where m_c and m_b are the quark masses and $M_B = 5.5$ GeV/c^2 is the mass of the lightest bottom flavored hadron.

E. M^o Heavy Lepton, Heavy Quark Production.

This type of mechanism for trimuon production was discussed previously by Barnett and Chang[7], and by Barger et al.,[8] who assumed the simultaneous production of a neutral heavy lepton M^o and a b quark. The decay $b \to u$ occurs with the emission of a μ^-. We assume that the dominant decay mode of the b quark is semi-leptonic and involves the emission of a c quark, namely

$$\begin{aligned} \nu_\mu + N \to\ & M^o + B + X \\ & \quad\ \ \lfloor\!\!\to C + \mu^- + \bar{\nu}_\mu \\ & \lfloor\!\!\to \mu^- + \nu_\mu + \mu^+ \end{aligned} \qquad (2.5)$$

which is depicted in Fig. 5. In this process four muons can be emitted if the charmed quark also decays leptonically. We assume that the mass of the M^o is in the range 2-4 GeV/c^2 but we illustrate our results only for the 4 GeV/c^2 case, with m_b=4.75 GeV/c^2 and m_c=1.5 GeV/c^2. If the quark transition were taken to be $b \to c + X$ followed by $c \to s + \mu^+ + \bar{\nu}_\mu$ then we would predict too many $\mu^-\mu^+\mu^+$ events which is incompatible with the present experimental results.

F. M^- Heavy Lepton Cascade.

In this process the trimuon events arise from the reaction

$$\begin{array}{l} \nu_\mu + N \to M^- + X \\ \qquad\qquad \hookrightarrow L^o + \mu^- + \bar{\nu}_\mu \\ \qquad\qquad\qquad \hookrightarrow \mu^- + \nu_\mu + \mu^+ \end{array} \tag{2.6}$$

illustrated in Fig. 6 and discussed in the literature at some length by the present authors[5] as well as by Barger et al.[6] Production of the M^- can be accompanied by either light or heavy quark production based on the particular gauge model one wishes to consider. We illustrate our results in Section III for the case of a $d \to u$ transition at the hadron vertex. The mass of the M^- is 8 GeV/c^2 and the mass of the L^o is set equal to 4 GeV/c^2. Results for the light-to-heavy quark transitions can be found in References 5 and 18. The multimuon event rates for the chain (2.6) depend on the M^- and L^o semileptonic branching ratios. One expects the $\mu^-\mu^-$ event rate to be larger than that for the $\mu^-\mu^-\mu^+$. In Reference 18 this question was examined in detail for one SU(3) x U(1) gauge model and the tetramuon event rate calculated. Also, the consequences of misidentifying events containing electrons and/or positrons was studied together with the effects of the minimum energy cuts on the muons. The latter effect is important when many muons are emitted and causes a large number of tetramuon events to be classified as trimuon events.

III. NUMERICAL COMPARISONS

In order to carry out numerical calculations, we adopt the parton model formalism and use the slow rescaling approach, where the scaling variable is

$$\xi_j = x + m_j^2/(2MEy) \tag{3.1}$$

in terms of $x = q^2/2M\nu$, $y = \nu/E$ and m_j, the mass of the heavy quark of type j. To treat the physical threshold correctly, we use $M_C = 2.25$ GeV/c^2 for the lightest charmed hadron $M_B = 5.5$ GeV/c^2 for the lightest bottom flavor hadron, and $M_T = 8.5$ GeV/c^2 for the top flavor hadron where we recall $m_c = 1.5$ GeV/c^2, $m_b = 4.75$ GeV/c^2 and $m_t = 7.5$ GeV/c^2 were chosen for the quark masses of the corresponding flavors.

To fold in the decay chains, it is necessary to make assumptions about the quark-parton model fragmentation functions $D_j^k(z)$ which give the probability that a quark of type j will convert into a hadron of type k, where $z = E_k/E_j$ is the ratio of the energy E_k carried by the hadron compared to the maximum allowed value. While the pion fragmentation functions $D^\pi(z)$ are found to fall off like $D^\pi(z) \cong (1-z)/z$, the functions are not anticipated to peak at z = 0 for heavier hadrons. In fact studies of the mass effects by Odorico,[19] Suzuki,[20] and Bjorken[21] suggest that, to a fair approximation, we can set

$$D^C(z) = 1.0$$

$$D^B(z) = \delta[z-(1 - \frac{M}{m_b})]$$

$$D^T(z) = \delta[z - (1 - \frac{M}{m_t})] \tag{3.2}$$

where m_b and m_t are the bottom and top quark masses and M is the nucleon mass.

For the values of the masses selected, the fractional energy distribution for the hadron from the B quark peaks at $z \gtrsim 0.8$ while that for the T peaks at $z \gtrsim 0.9$. In semileptonic decays of the hadrons, the muons can thus be emitted with relatively high energies.

We now proceed to give some distributions for the processes under consideration. It is impractical to publish all the possible correlations between the three muons and the final hadrons. We have studied them to select the most discriminating. In general the single differential distributions which are the most helpful are the production cross sections, the energy distributions of the muons and hadrons, the invariant masses of the pairs, the transverse momenta perpendicular to the neutrino direction and to the plane containing the fast μ^- and the ν, and the azimuthal correlations in the plane perpendicular to the neutrino beam. We distinguish the two negative muons by binning them into fast and slow according to their energy and call $E_1 = E_{\mu^-,\text{fast}}$, $E_2 = E_{\mu^-,\text{slow}}$ and $E_3 = E_{\mu^+}$ in the usual way. All the distributions are given after weighting by the FHPRW quadrupole triplet spectrum.

A. Cross Sections and Threshold Effects.

The production cross sections for the six reactions we consider have different characteristics. For example, the threshold for the radiative process is very low, apart from the fact that the muons must be produced with sufficient energies to be dectected ($E_\mu \gtrsim 4$ GeV). The other reactions have different thresholds depending on the masses of the particles involved. For the production of heavy leptons in particular, the threshold can be pushed relatively high if they are only produced in association with heavy quarks. Higgs meson masses are generally unknown and ould be as light as 3-4 GeV/c^2. If this is true then the threshold for Higgs boson production can also be rather low.

remarks by giving the energy dependences of the production cross sections in Fig. 7 for the masses chosen above. In order to distinguish more easily between the different models we follow the convention that results from models A (radiative) and D (diffractive) are shown with solid lines, results from models B (Higgs) and E (M^2-hadron) are shown with dashed lines and results from models C (hadron cascade) and F (lepton cascade) are shown with dot-dashed lines. In Figure 7 we also show the regular single muon inclusive cross section which rises linearly with the beam energy E. The cross sections have not been folded by the neutrino flux distribution. The radiative cross section has the lowest threshold and increases like $E \log^2 E$ for large values of the beam energy. The cross sections for B and D increase with E quadratically. All the other cross sections are asymptotically linear in E ; however , because we have chosen large masses for the quarks and leptons, these asymptotes are only reached beyond the energies atainable at Fermilab and CERN.

In Fig. 8 we show the visible energy distribution when the cross sections are folded by the FHPRW quadrupole triplet wide-band spectrum. Note that the E_{vis} distributions for models C,D,E and F are not the same as the $\sigma \times$ flux plots because there are always two neutrinos which carry away some energy. This systematically lowers the energies of the events and makes the reactions appear to have smaller thresholds. The present data from the FHPRW group consist of eleven $\mu^-\mu^-\mu^+$ events where all the muon energies are measured. However, the hadron energies are only known for four of the events so the visible energy of the other events is larger than the sum of the three muon energies by an unknown amount. We give a histogram plot of the visible energies of the FHPRW data in Fig. 9 and cross hatch those events where the hadron energy is unknown. It is clear that the distribution of trimuon events versus the total visible energy will reflect both the threshold behavior and the asymptotic values of the cross sections. With a reasonable increase in statistics it will be possible to see if there is any hint of an energy threshold. However a word of caution is necessary at this point. If heavy lepton and/or heavy quark models are the explanation of some of the trimuon events then there will be missing neutrinos so the total energy in each event will only be accurately determined in a narrow band dichromatic beam experiment.

B. Energy Distributions.

In Fig. 10, we show the energy distributions of the three muons for the models and the distributions in the hadron energies. Figure 11 gives the corresponding histograms of the FHPRW data. It is impractical to add all six theoretical predictions to the graphs with the data so we present them separately. Our curves for the distributions are not scaled in any particular way as we have not tried to normalize the event rates. Clearly the μ^+ tends to be rather slow when it arises from the decay of a massive quark. The ordering of the two μ^- particles into μ^-_{fast} and μ^-_{slow} generally makes the slow μ^- have a lower average energy than the μ^+. In most models the slow μ^- and the μ^+ have a reasonable probability that they will not escape the experimental minimum energy cut ($E_\mu \gtrsim 4$ GeV) so genuine trimuon events will therefore be registered as $\mu^-\mu^+$ or $\mu^-\mu^-$ events. The opposite sign dimuon pairs may not stand out from the signal caused by the decays of charmed particles; however, the $\mu^-\mu^-$ events should be detected and will provide good evidence for or against a particular model.

From Fig. 10 one sees that the hadronic energy distribution will help to differentiate between the models. The diffractive model (D) gives soft muons and a hard hadron spectrum. Also the hadronic cascade model (C) is very effective in producing energetic hadrons accompanied by soft muons. The double differential distributions in the energies, to be presented later, show these features very clearly.

C. Invariant Mass Plots.

The invariant mass plots shown in Fig. 12 make precise the general features expected from qualitative arguments and should be compared with the data given in Fig. 13. When the muons are produced in heavy lepton (or heavy quark) decays then the M_{123} distribution cannot be larger than the mass of the heaviest lepton (or particle carrying the quantum numbers of the quark). However, if the muons are produced in different decay chains then there is no corresponding limit on the trimuon invariant mass. Thus, if no events are found with masses larger than say 6 GeV/c^2 then the M^o-hadron model as well as the Higgs particle model will probably have to be excluded as the only source of the trimuon events. The distributions in the invariant masses of the pairs also contain valuable information. Obviously the M_{23} invariant mass provides a decisive test of radiative versus non-radiative processes. The electromagnetic production shows a typical bremsstrahlung spectrum which is bounded at small masses by the sum of the masses of the two muons. In contrast the Higgs boson case yields a dramatic peaking in the M_{23} invariant mass (assuming a two body decay into $\mu^+\mu^-$). This feature can be exploited to bound the mass of the Higgs particle using models to calculate the branching ratio $H \to \mu^+\mu^-$.

D. Transverse Momenta.

The transverse momenta perpendicular to the neutrino direction or perpendicular to the plane containing the fast μ^- and the W^+ contains valuable information on whether the other muons are produced in a point-like fashion. Both the hadronic cascade and the leptonic cascade mechanisms yield muons with large transverse momenta. In Fig. 14 we show the transverse momentum spectra relative to the direction of the neutrino beam. The histograms showing the corresponding results for the FHPRW events are shown in Fig. 15. We complement this information by giving the theoretical transverse momenta of both the slow μ^- and the μ^+ with respect to the plane containing the neutrino and the fast μ^- in Fig. 16. The corresponding data are shown in Fig. 17. The latter distributions are all peaked at rather low values of $p_\perp$.

E. Azimuthal Angles.

Other key correlations in distinguishing between production mechanisms are the azimuthal angles between pairs of dimuon transverse momenta projected on the plane perpendicular to the neutrino beam. The results for the models discussed in the text are given in Fig. 18, while the data are shown in Fig. 19. The ϕ distributions are unfortunately rather difficult to measure accurately so we must await more events before any firm conclusions can be drawn.

The ϕ_{12} angle between the projections of the two negative muons contains valuable information on whether the second muon arises from the leptonic side of the interaction or the hadronic side. Hadronic cascade decay models yield muons which are directed along the direction of the hadron jet so ϕ_{12} peaks at 180^o. This correlation is clearly present in the opposite sign dimuon events arising from the production and decay of charmed particles.[22] The ϕ angles in the radiative process have more structure which reflects the cancellation among the terms in the matrix element due to gauge invariance. The forward peaking is due to radiation from the muon and the backward peaking is caused by radiation from the hadrons (quarks).

F. Double Differential Distributions.

We have examined several double differential distributions. One plot we found to be very useful is a scatter plot of E_1-E_{had} versus E_2+E_3. Rather than draw actual scatter plots we present the same information by giving the number of events (normalized to approximately one thousand events) in bins of 40 GeV versus 15 GeV in Figs. 20-25. This information also helps to evaluate the probability of explaining the extremely energetic events seen at Fermilab by the FHPRW group. These events have E_1-E_{had} values of ~150 GeV and ~70 GeV while the E_2+E_3 values are ~75 GeV and ~155 GeV respectively. We have added the measured points to the scatter plots as dots (when the hadron energy is measured) and lines (when E_{had} is not known). In general E_{had} cannot be too large otherwise the hadronic shower would punch through the iron in the FHPRW experiment and be detected.

In Fig. 20 we give the results for model A. Clearly the probability of producing events with $E_2 + E_3 \gtrsim 60$ GeV is very small. The situation is much better in the case of Higgs boson production as illustrated in Fig. 21. Figure 22 shows the scatter plot for the hadron cascade model, where both the secondary muons are rather soft. In this model E_{had} tends to be larger than E_1 so most of the events fall in the region where $E_1 - E_{had}$ is negative. This latter feature is even more pronounced in the scatter plot for the diffractive model given in Fig.23. However, if we turn to the M^0- hadron model then the secondary muons tend to be almost as fast as the primary (i.e., fast) μ^- and the distribution of events changes dramatically. This model has some events in the regions where the energetic events fall but again the probability is very small. Finally the results are given for the heavy lepton cascade model in Fig. 25. This model was constructed to give fast muons and one can obtain $E_2 + E_3$ values as large as 70 - 80 GeV with a small probability.

The second correlation we present is that of E_{had} versus the energy of the slowest muon $E_{slowest}$. The latter can have either charge. In the next series of plots from Fig. 26 to Fig. 31 we show this two dimensional correlation for the models in bins of 10 GeV by 40 GeV and add the data points from the FHPRW experiment. The hadron cascade model (Fig. 28) and the diffraction model (Fig. 29) clearly have different distributions of events from those of the other four models. Figures 26-31 are also helpful in assessing the probability of finding super events but unfortunately E_{had} is not known for event number 281-147196. However, the sum of the muon energies is already 260 GeV for this event so E_{had} is unlikely to be larger than 40 GeV. Clearly it is very difficult to find any explanation of an event where $E_{slowest}$ is as large as 70 GeV. We remind the reader that the neutrino spectrum falls off rather sharply in the region around 300 GeV. A close examination of Figures 20-31 shows that most events have measured energies in reasonable agreement with the predictions of the models but some fall outside the allowed regions. More events are required before definitive statements can be made.

In summary, none of the models are really successful in explaining the two super events. Even though the angles and $p_\perp$ correlations for these events are not a problem, the energies seem anomalously large. As we can see from Figs. 20-31, the super events are completely outside the boundary of the scatter plots for some of the models. In the other cases they are very close to the edge of the scatter plot, which indicates that they occur with very low probability. If the latter models have any hope of explaining the trimuon events, then many more normal events should have been detected. The models with the most favorable probability of explaining the super events are the radiative model and the Higgs model. However, the Higgs model does not give any reasonable fit to the M_{23} spectrum.

IV. CONCLUSIONS

We have concentrated on neutrino production of trimuon events and presented single and double differential distributions to distinguish between the models A–F, namely, radiative production of muon pairs, Higgs boson production and decay, hadron(quark) cascade, diffractive production of a pair of heavy quarks, M^o-hadron decays, and M^- cascade decays respectively. The distributions have been flux averaged with the FHPRW quadrupole triplet spectrum. The results we have given above should allow a weeding out of possible models once more data is available. The radiation of muon pairs (model A) is expected to occur with an event rate $\sigma(3\mu)/\sigma(\mu) \sim 2\times10^{-5}$ when we incorporate experimental cuts. The experimental results for M_{23} already show a peaking in this variable, and cuts can be made to remove this process. To find other signals we see that the M_{23} invariant mass distribution is a precise test of model B while the M_{123} invariant mass distribution will put limits on model E. The models C and D lead to spectra in E_{had}, which peak at large energies and cannot account for the super-events which must have small E_{had} energies. Heavy lepton cascade models, and in particular model F, yield muons with large transverse momenta perpendicular to the neutrino direction. The azimuthal angular distributions between pairs of muons also discriminate between leptonic and hadronic cascade mechanisms.

Trimuon production rates have not been emphazised here because in general they are highly model dependent. The one exception to this rule is the electromagnetic production of muon pairs. However, even in this case, it is not clear that <u>all</u> important Feynman diagrams are included. For instance quark-antiquark annihilation into virtual photons, which convert into muon pairs, has not been analysed and is probably important for dimuon pairs with large invariant mass. The estimate given in Ref. 13 is certainly very reasonable but we must remember that the predicted rate appears to be too small to account for the experimental rate so other mechanisms are probably also present. The production cross section for model B(Higgs scalar) can be calculated reliably but it is difficult to estimate the branching ratio for $H \rightarrow \mu^+\mu^-$. While the electromagnetic production of vector mesons has been shown to be too small to fit the observed rate,[12] the hadronic production may be so large that it could account for some of the events. In that case the M_{23} invariant mass distribution will show peaks at the position of the vector meson masses. Both models A and B differ from the other four with respect to their E_{tot} distributions. However, due to the fact that there are missing neutrinos in models C,D, E and F, E_{tot} cannot be measured accurately. The visible energy distributions may allow one to distinguish model A from the other models. A careful study using a dichromatic beam can check whether the trimuon events have missing energy.

Several other tests of these models can be made using rates for the antineutrino production of $\mu^+\mu^+\mu^-$ events and neutrino/antineutrino production of same sign dimuon and opposite sign dimuon events. The most obvious tests involve only measurements of rates. For instance, suppose that the neutrino production of $\mu^-\mu^-$ events has a larger rate than the neutrino production of $\mu^-\mu^-\mu^+$ events. If this is true then models C,D,E, and F with new heavy leptons and/or heavy quarks would be favored because these new particles have presumably larger nonleptonic branching ratios than semi-leptonic branching ratios. Both the FHPRW and CDHS groups have detected $\mu^-\mu^-$ events[2,23] but it is not a trivial problem to understand if there is a genuine signal above the background from pion and kaon decays so unfortunately the present situation is rather unclear. However, if the $\mu^-\mu^-$ signal turns out to be smaller than the signal for the $\mu^-\mu^-\mu^+$ events, then models which will be favored are the electromagnetic and the Higgs boson. In both cases one should only see $\mu^-\mu^-\mu^+$ but there is a reasonably large probability that the μ^+ will not survive the energy cut so some trimuon events will be registered incorrectly as $\mu^-\mu^-$ events. The existence and magnitude of a $\mu^-\mu^-$ signal is very important and hopefully we should know the answer rather soon. Misidentified trimuon events of the $\mu^-\mu^+$ type will also occur but they will be very difficult to observe due to the large rate for these events arising from the production and decay of charmed particles.

The search should also be continued for opposite sign trimuons, i.e., ν produced $\mu^-\mu^+\mu^+$ events, and for tetramuons produced in neutrino beams. The rates for these processes also impose restrictions on the possible gauge models with heavy leptons and/or heavy quarks. However experimental acceptances and cuts have to be incorporated very carefully for such multimuon processes because the muons are so soft that events are misclassified.

The presently available antineutrino beams are much less intense than the neutrino beams so absolute rates for trimuon production are correspondingly smaller. In the models considered above there are important helicity effects which reduce the antineutrino cross sections relative to the neutrino cross-sections. For instance the $\bar{\nu}$ production of $\mu^+\mu^+\mu^-$ events in model A has the same rate relative to the $\bar{\nu}$ production of μ^+ events as the corresponding rates for ν beams. However the $\bar{\nu}$ cross section is reduced by the usual factor of three relative to the ν cross section. In terms of event rates this factor is larger due to the absence of good $\bar{\nu}$ beams. Model D also has favorable $\bar{\nu}$ event rates because diffractively produced quark pairs have equal ν and $\bar{\nu}$ cross sections. However models B,C,E and F may have low $\bar{\nu}$ rates due to both the helicity effects at the production vertices and the poor $\bar{\nu}$ beams. Nevertheless, even if it is difficult to find $\bar{\nu}$ induced events most models would prefer them to be with the charge combination $\mu^+\mu^+\mu^-$. Production of $\mu^-\mu^+\mu^+$ events in a ν beam or alternatively production of $\mu^+\mu^-\mu^-$ events in $\bar{\nu}$ beam would necessitate a change in our attitude towards trimuons.

Most of the emphasis in this paper has been on the production of multi-muon events because the counter experiments cannot detect electrons or positrons. However bubble chamber exposures should see $\mu^- e^- e^+$ events arising from model A. Searches should also be made for other exotic charge combinations such as $\mu^- \mu^+ e^-$ or $\mu^- e^-$. Event rates for these reactions can be estimated for models C to F. If models A or B are correct then these signatures can only come from background processes.

Note: While this paper was being prepared we received a preprint from R. M. Barnett, L-N Chang and N. Weiss [SLAC-PUB-2063] which also contains a comparison of different trimuon production models. We thank these authors for sending their results to us prior to publication.

ACKNOWLEDGEMENTS

This work has been supported in part by the National Science Foundation under Grant Nos. Phys. 77-07864 and 76-15328 and by the Department of Energy. We would like to thank the members of the FHPRW group for discussions on their data.

REFERENCES

[1]B. C. Barish, et al., Phys. Rev. Letters 38 577 (1977).

[2]A. Benvenuti , et al., Phys. Rev. Letters 38 1110 (1977); See also talk by D. Reeder at the 1977 International Symposium on Lepton and Photon Interactions at High Energy. A. Benvenuti, et al., University of Pennsylvania Preprint.

[3]M. Holder, et al., Phys. Lett. 70B,393 (1977).

[4]See reports by D. Cline and by J. Steinberger at the 1977 Irvine Meeting.

[5]A. Benvenuti, et al., Phys. Rev. Letters 38 1183 (1977); C.H.Albright, J.Smith and J.A.M.Vermaseren, Phys. Rev. Letters 38 1187 (1977); Phys. Rev. D16, 3182, 3204 (1977).

[6]V. Barger, T. Gottschalk, D.V.Nanopoulos, J.Abad and R.J.N.Phillips, Phys. Rev. Letters 38 1190 (1977), Phys. Rev. D16 2141 (1977).

[7]R.M.Barnett and L-N.Chang, Phys. Lett. 72B, 233 (1977).

[8]V. Barger, T. Gottschalk and R.J.N. Phillips, Phys. Lett. 70B, 243 (1977).

[9]F. Bletzacker, H. T. Nieh and A. Soni, Phys. Rev. Letts. 38, 1241 (1977); F. Bletzacker and H. T. Nieh, Stony Brook preprint ITP-SB-77-42.

[10]H. Goldberg, Phys. Rev. Lett. 39, 1598, (1977).

[11]A. Soni, Phys. Lett. 71B, 435 (1977).

[12]R. Godbole, Stony Brook preprint ITP-SB-77-70.

[13]J. Smith and J.A.M. Vermaseren, Stony Brook preprint ITP-SB-77-66;

[14]V. Barger, T. Gottschalk and R.J.N. Phillips, University of Wisconsin preprint COO-881-9.

[15]P. Langacker and G. Segre, Phys. Rev. Lett. 39, 259 (1977).
P. Langacker, G. Segre and M. Golshani, UPR-0079 T.

[15](continued) B. W. Lee and S. Weinberg, Phys. Rev. Lett. 38, 1237 (1977).

B. W. Lee and R. E. Shrock, Fermilab-Pub. 77/48-THY.

D. Horn and G. G. Ross, Phys. Letts. 69B, 364 (1977)

V. Barger, D. V. Nanopoulos and R. J. N. Phillips, University of Wisconsin preprint COO-597(1977).

A. Zee, F. A. Wilczek and S. B. Treiman, Phys. Letts. 68B, 369 (1977).

S. Pakvasa, H. Sugawara and M. Suzuki, Phys. Letts. 69B, 461 (1977).

A. DeRujula, H. Georgi and S.L. Glashow, Harvard preprint 77/A028.

V. K. Cung and C. W. Kim, Phys. Lett. 69B, 359 (1977).

G. C. Branco, S. Nandi, H. P. Nilles and V. Rittenberg, BN-HY-77-9.

J. Ellis, M. K. Gaillard, D.V.Nanopoulos and S. Rudaz, Nucl.Phys. B131, 285 (1977).

Review articles have been written by

R. M. Barnett, SLAC-PUB-1961 (1977) and by

V. Barger, University of Wisconsin preprint COO-881-7.

[16]A. M. Cnops, et al., Phys. Rev. Lett. 40, 144 (1978).

[17]M. Perl, et al., Phys. Rev. Letts. 35, 1489 (1975); Phys. Letts. 63B, 466 (1976).

[18]C. H. Albright, R. E. Shrock and J. Smith, Fermilab-Pub-77/81 Th.

[19]R. Odorico, Phys. Letts. 71B, 121 (1977).

R. Odorico and V. Roberto, CERN preprint Th-2431 (1977).

[20]M. Suzuki, Phys. Letts. 71B, 139 (1977).

[21]J. D. Bjorken, SLAC-PUB-1992 (1977).

[22]M. Holder, et al., Phys. Lett. 69B, 377 (1977).

[23]M. Holder, et al., Phys. Lett. 70B, 396 (1977).

FIGURE CAPTIONS

Fig. 1. Feynman diagrams for the radiative production of muon pairs.

Fig. 2. Feynman diagram for the production and decay of a Higgs boson.

Fig. 3. Feynman diagram for the heavy quark cascade decay.

Fig. 4. Feynman diagram for the diffractive production and decay of a pair of heavy quarks.

Fig. 5. Feynman diagram for the production and decay of a neutral heavy lepton and a heavy quark.

Fig. 6 Feynman diagram for the charged heavy lepton cascade decay.

Fig. 7 Production cross sections for the six models considered in this paper. We use solid lines for the results of models A and D, dashed lines for models B and E, and dot-dashed lines for models C and F. The single μ^- inclusive cross section is also shown for comparison.

Fig. 8. E_{vis} distributions for the six models considered. The notation is the same as in Fig. 7.

Fig. 9. Histograms of the visible energies for the FHPRW events. Those events which are hatched do not have a measured E_{had}.

Fig.10. Energy distributions for the six models. The notation is the same as in Fig. 7.

Fig.11. Histograms of the energy distributions for the FHPRW events.

Fig.12. Distributions in the invariant masses. The notation is the same as in Fig. 7.

Fig.13. Histograms of the invariant masses for the FHPRW events.

Fig.14. Distributions in the transverse momenta perpendicular to the direction of the neutrino beam. The notation is the same as in Fig. 7.

Fig.15. Histograms of the transverse momenta perpendicular to the direction of the neutrino beam for the FHPRW events.

Fig.16. Distributions in the transverse momenta of the slow μ^- and the μ^+

FIGURE CAPTIONS (continued)

Fig. 16. perpendicular to the plane of the ν and the fast μ^-. The notation is the same as in Fig. 7.

Fig. 17. Histograms of the transverse momenta of the slow μ^- and the μ^+ perpendicular to the plane of the ν and the fast μ^- for the FHPRW events.

Fig. 18. Distributions in the azimuthal angles between the muons in the plane perpendicular to the direction of the neutrino beam. The notation is the same as in Fig. 7.

Fig. 19. Histograms of the azimuthal angles between the muons in the plane perpendicular to the direction of the neutrino beam for the FHPRW events.

Fig. 20. Number of events in a two-dimensional scatter plot of $E_2 + E_3$ (in GeV) versus $E_1 - E_{had}$ (in GeV) for model A (electromagnetic production). The total number of events is normalized to approximately one thousand. The dots represent the FHPRW events where E_{had} is measured and the lines the FHPRW events where E_{had} is not measured.

Fig.21. Same as Fig. 20 for model B (Higgs production).

Fig.22. Same as Fig. 20 for model C (hadron cascade).

Fig.23. Same as Fig. 20 for model D (diffractive production).

Fig.24. Same as Fig. 20 for model E (M^o-hadron).

Fig.25. Same as Fig. 20 for model F (heavy lepton cascade).

Fig.26. Number of events in a two-dimensional scatter plot of $E_{slowest}$ (in GeV) versus E_{had} (in GeV) for model A (electromagnetic production). The total number of events is normalized to approximately one thousand. The dots represent the FHPRW events where E_{had} is measured and the lines the FHPRW events where E_{had} is not measured.

Fig.27. Same as Fig. 26 for model B (Higgs production).

Fig.28. Same as Fig. 26 for model C (hadron cascade).

Fig. 29. Same as Fig. 26 for model D (diffractive production).

Fig. 30. Same as Fig. 26 for model E (M^o hadron).

Fig. 31. Same as Fig. 26 for model F (heavy lepton cascade).

Fig. 1

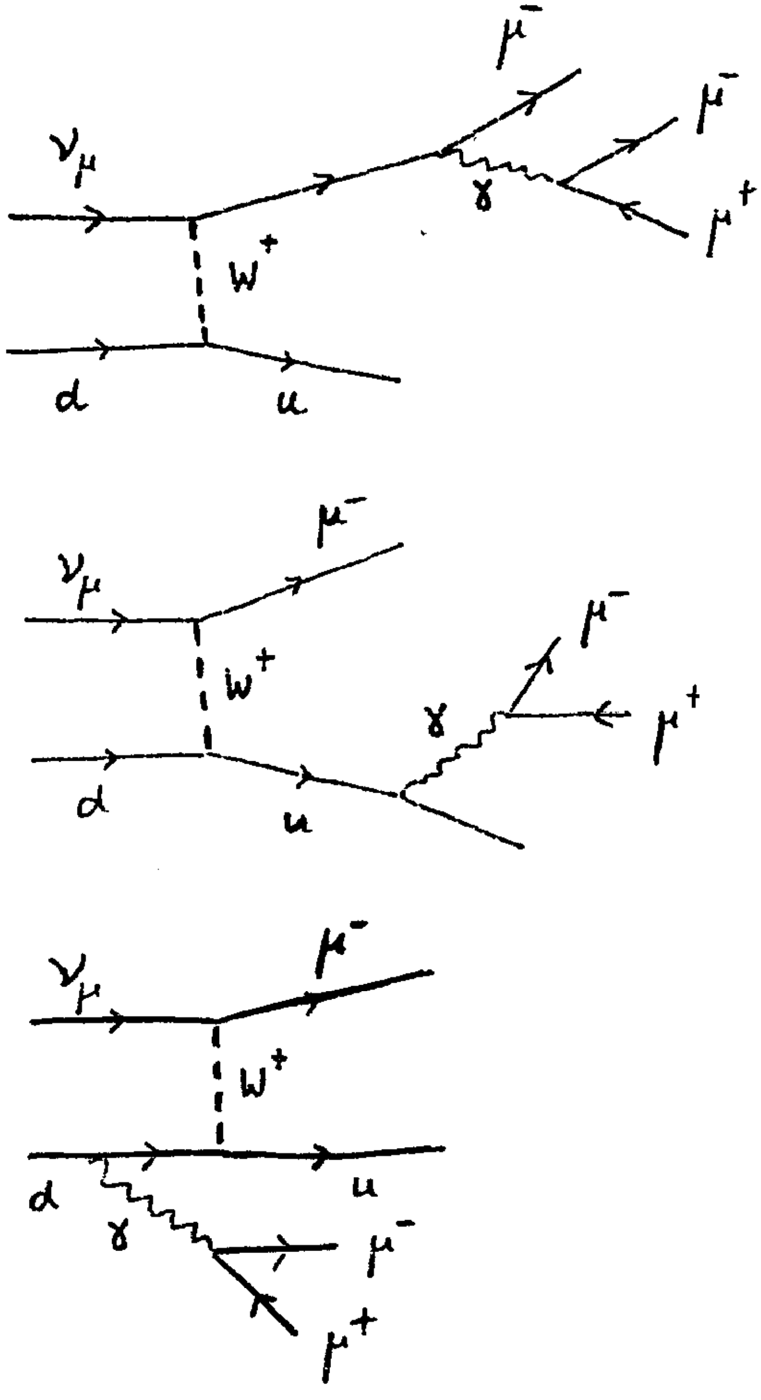

ν_μ
μ^-
μ^-
γ
μ^+
W^+
d
u
ν_μ
μ^-
W^+
μ^-
γ
μ^+
d
u
ν_μ
μ^-
W^+
d
u
γ
μ^-
μ^+

Fig.2

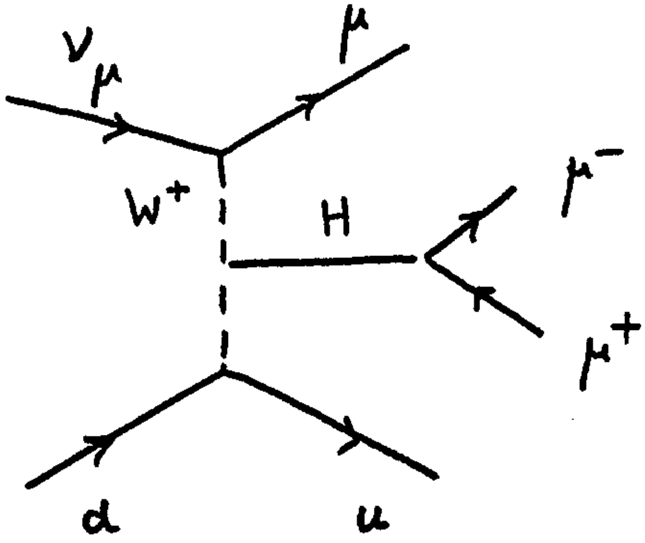

Fig. 3

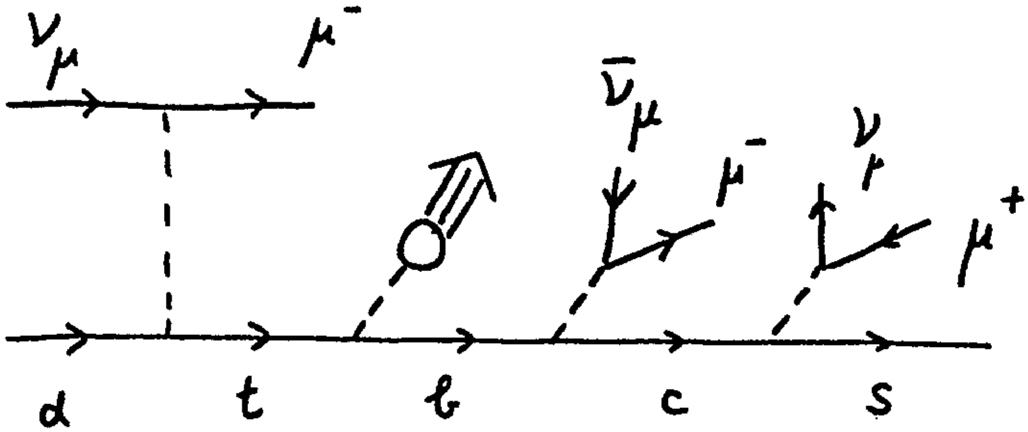

Fig. 4

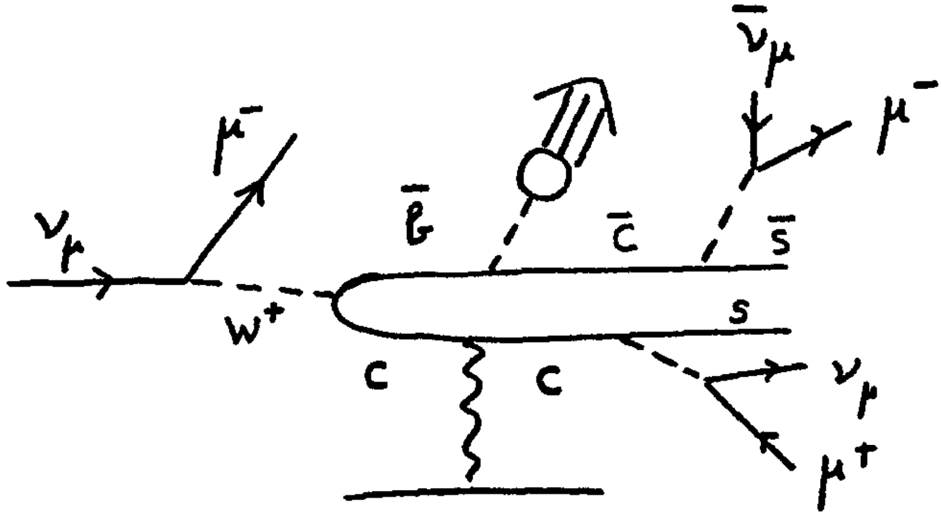

$\bar{\nu}_\mu$
μ^-
μ^-
ν_μ
$\bar{b}$
$\bar{c}$
$\bar{s}$
W^+
s
c
c
ν_μ
μ^+

Fig. 5

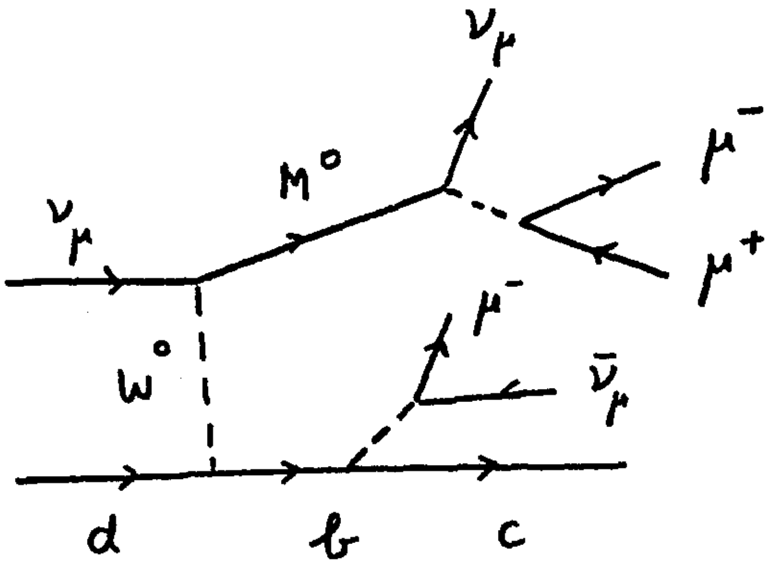

ν_μ
M^0
μ^-
ν_μ
μ^+
μ^-
W^0
$\bar{\nu}_\mu$
d
b
c

Fig.6

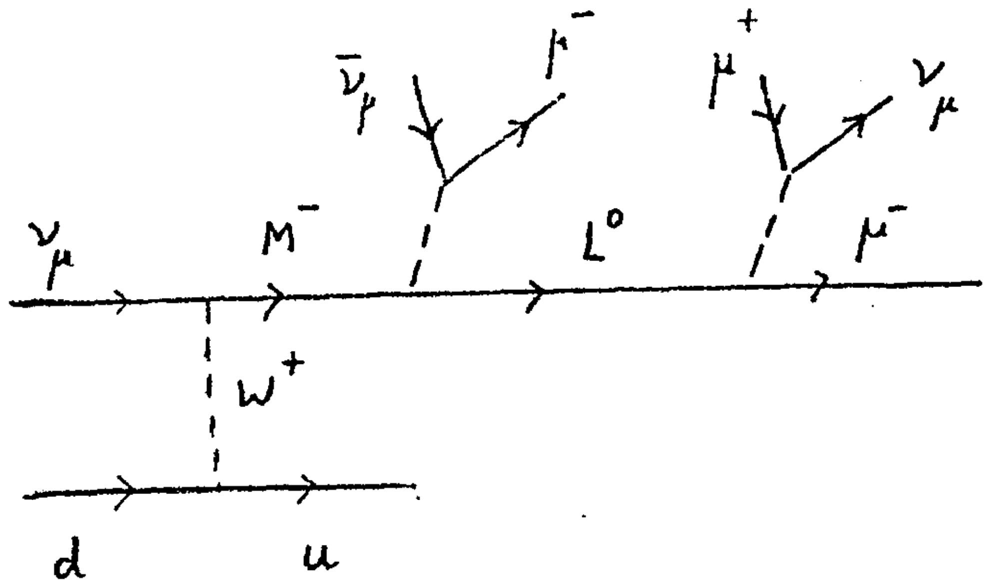

Fig.7

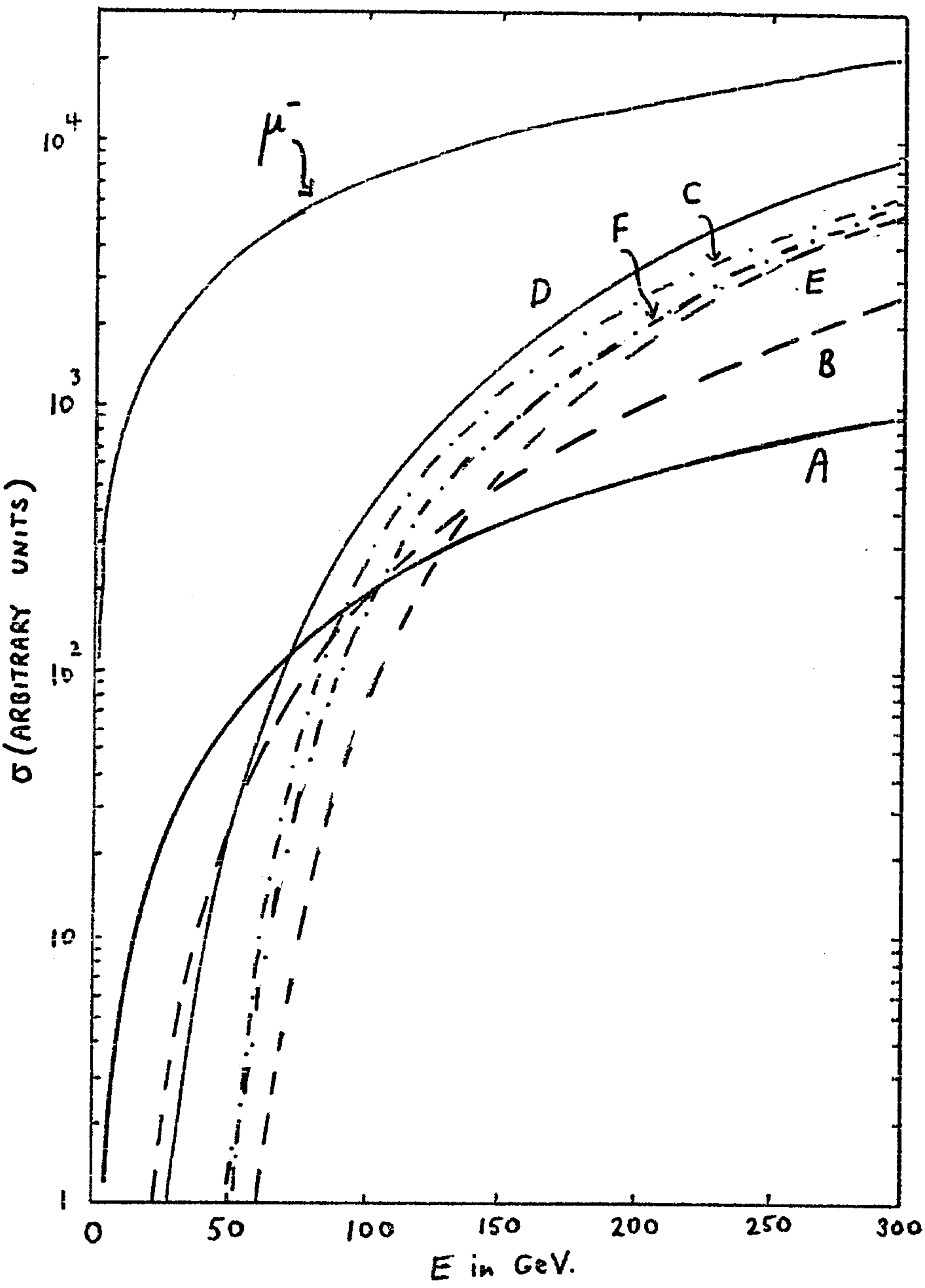

10^4
10^3
10^2
10
1
σ (ARBITRARY UNITS)
0
50
100
150
200
250
300
E in GeV.
μ⁻
C
F
D
E
B
A

Fig. 8

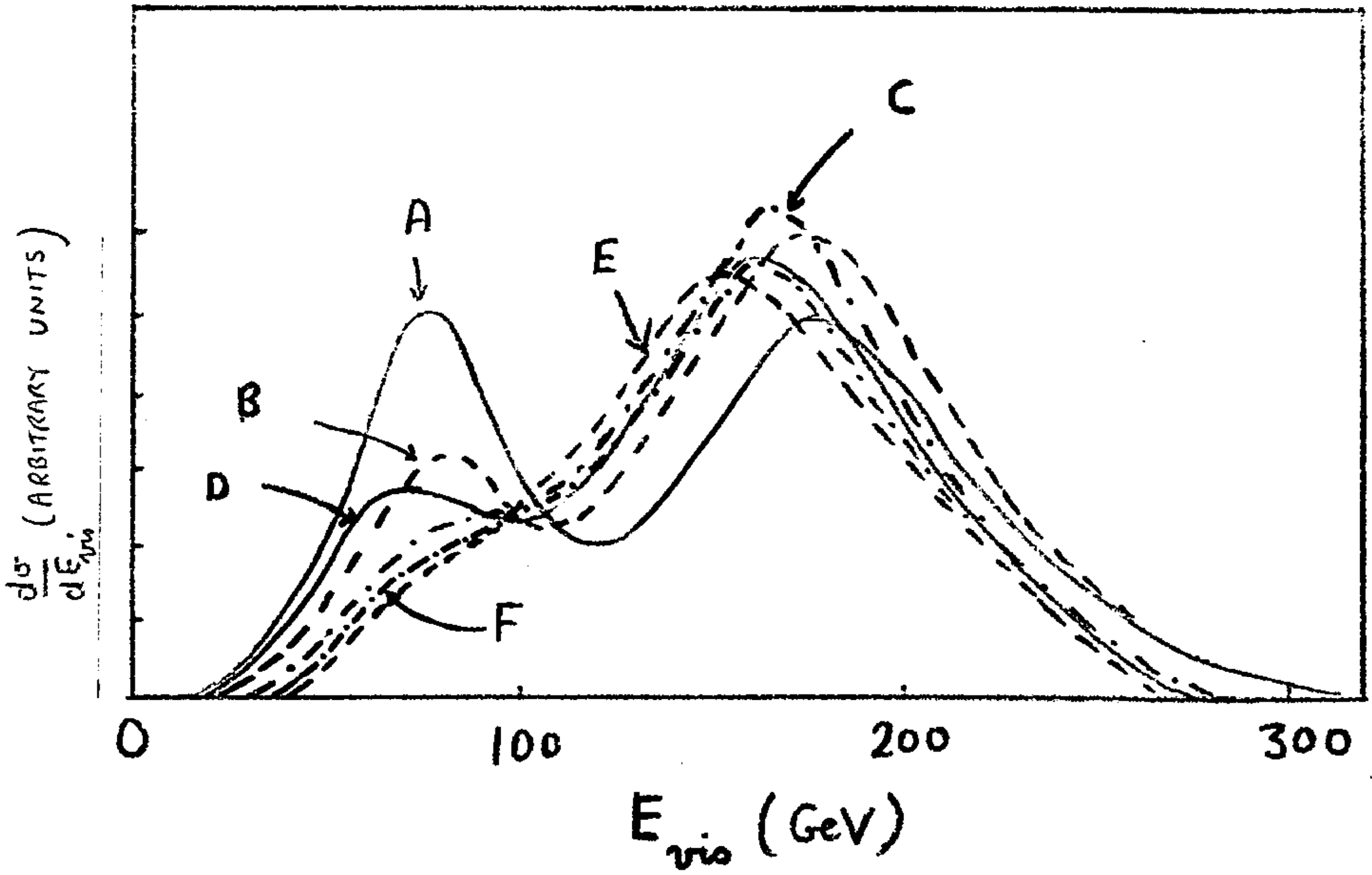
A
B
C
D
E
F
dσ/dE_vis (ARBITRARY UNITS)
0
100
200
300
E_vis (GeV)

Fig. 9

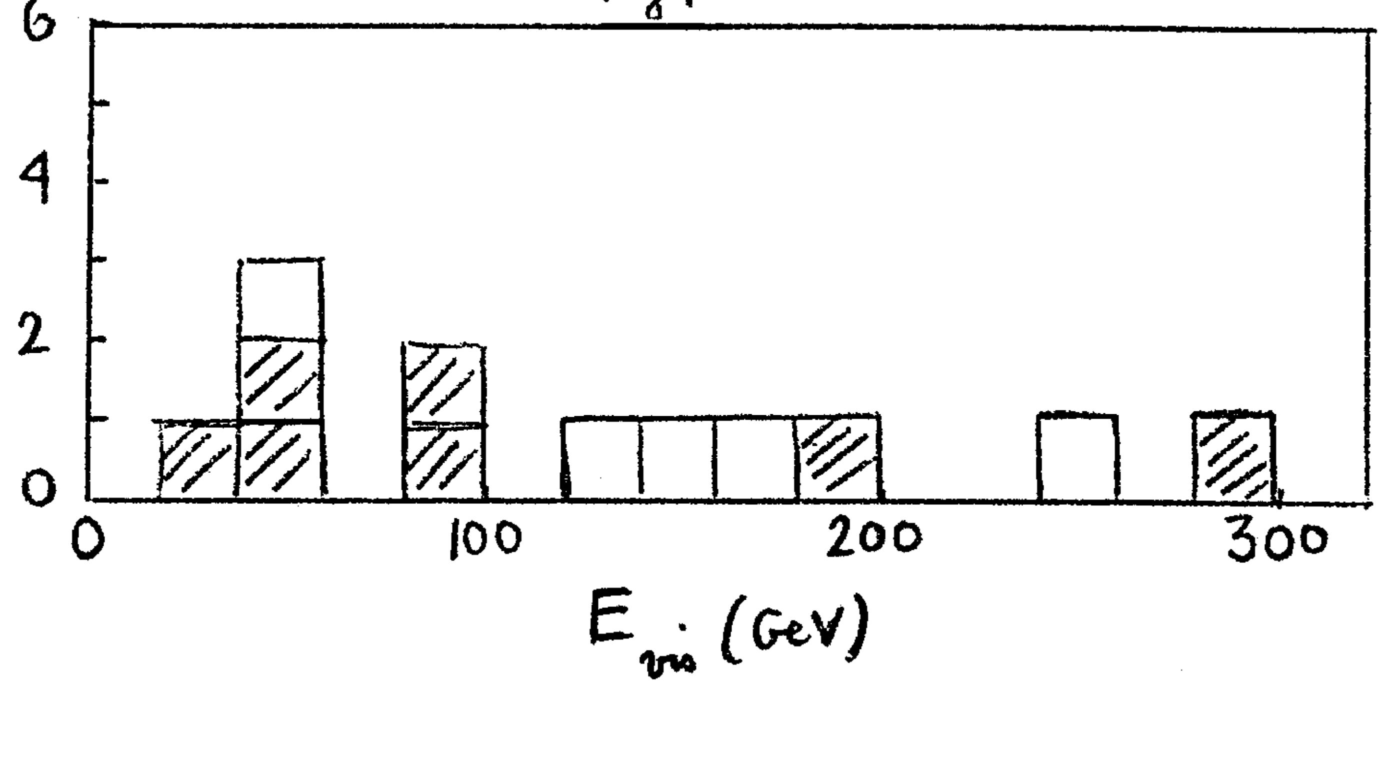
6
4
2
0
0
100
200
300
E_vis (GeV)

Fig. 10

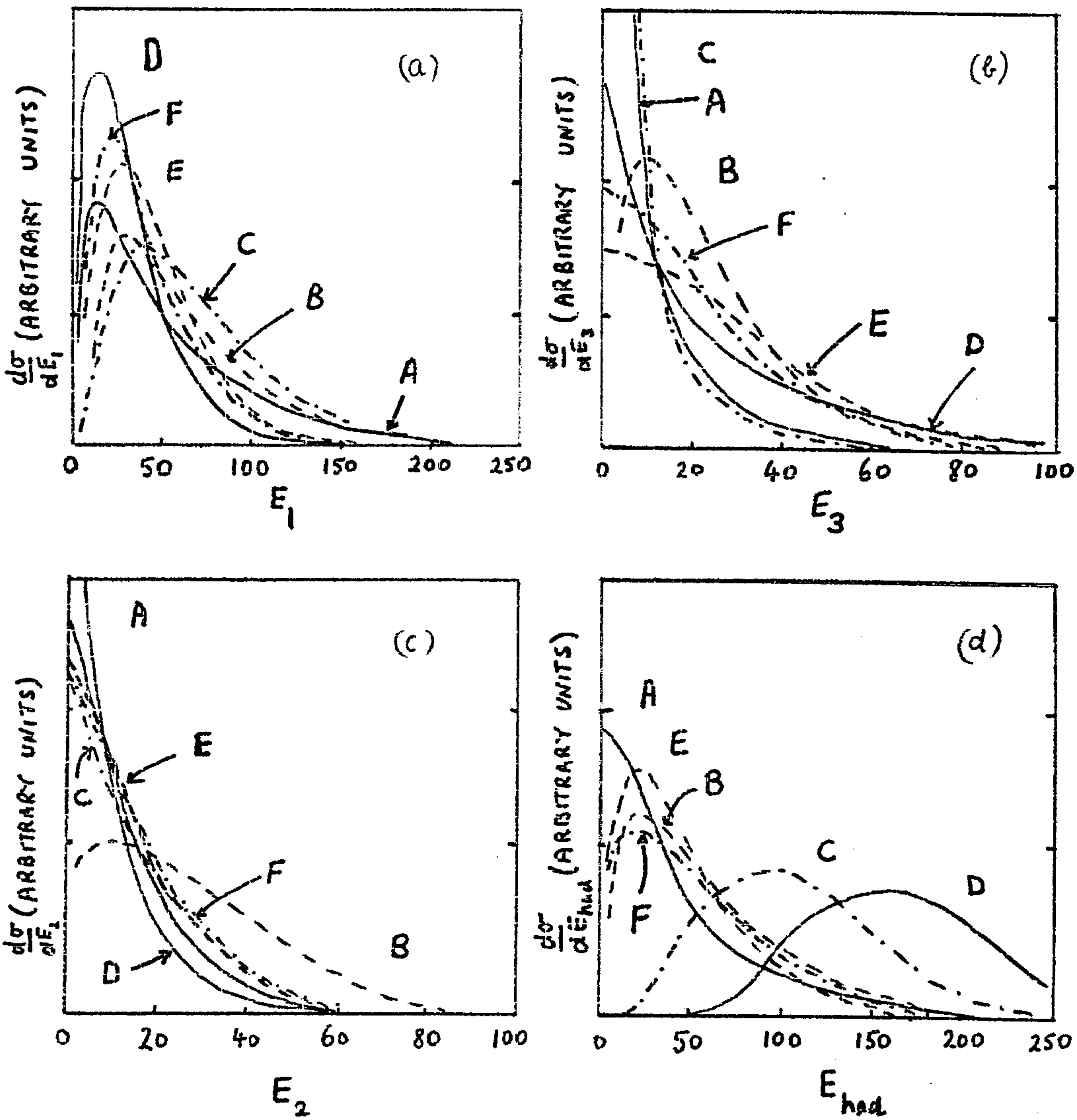

(a)
D
F
E
C
B
A
0
50
100
150
200
250
E_1
$\frac{d\sigma}{dE_1}$ (ARBITRARY UNITS)
(b)
C
A
B
F
E
D
0
20
40
60
80
100
E_3
$\frac{d\sigma}{dE_3}$ (ARBITRARY UNITS)
(c)
A
E
C
F
D
B
0
20
40
60
80
100
E_2
$\frac{d\sigma}{dE_2}$ (ARBITRARY UNITS)
(d)
A
E
B
F
C
D
0
50
100
150
200
250
E_{had}
$\frac{d\sigma}{dE_{had}}$ (ARBITRARY UNITS)

Fig 11

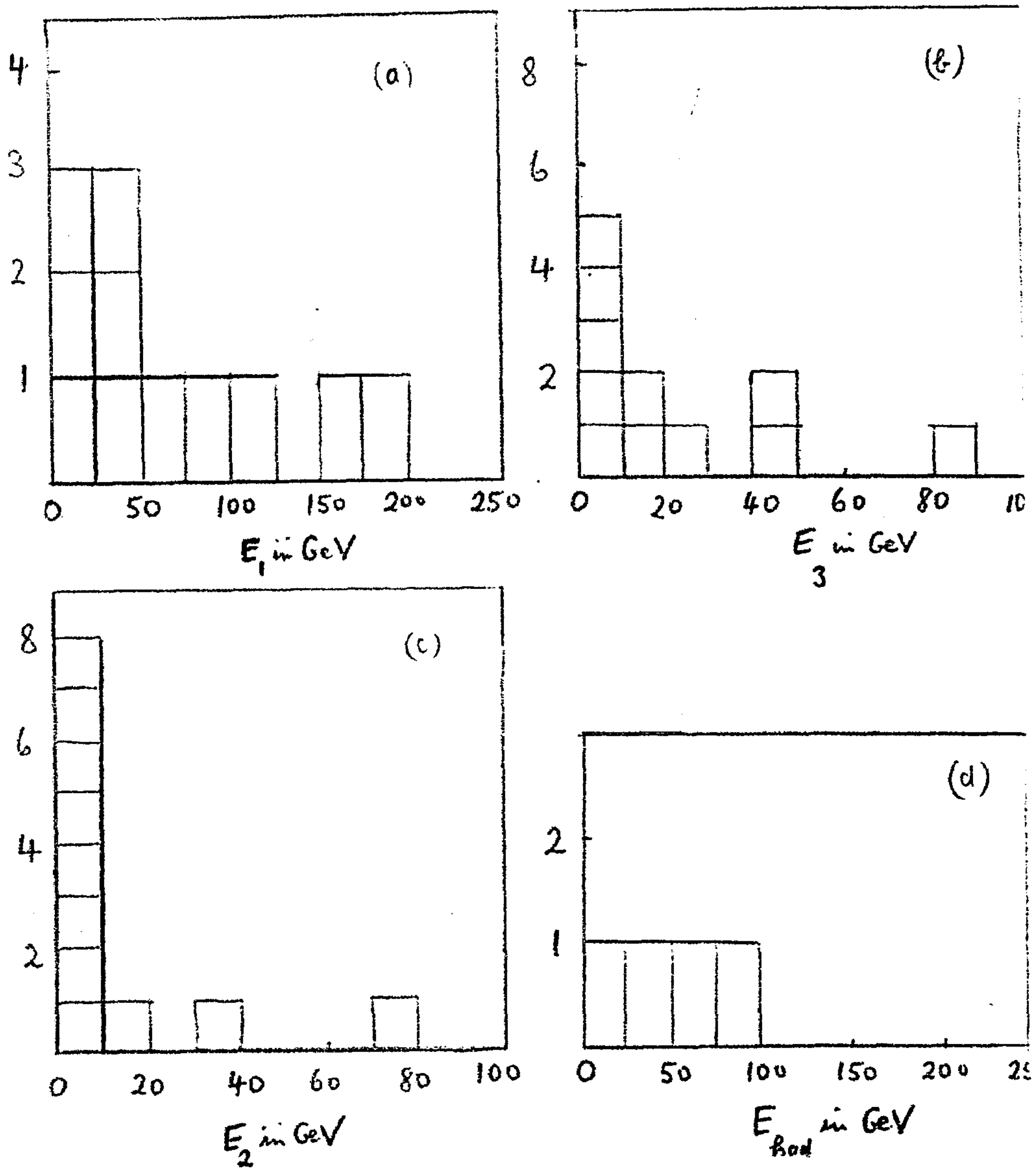

Fig. 12

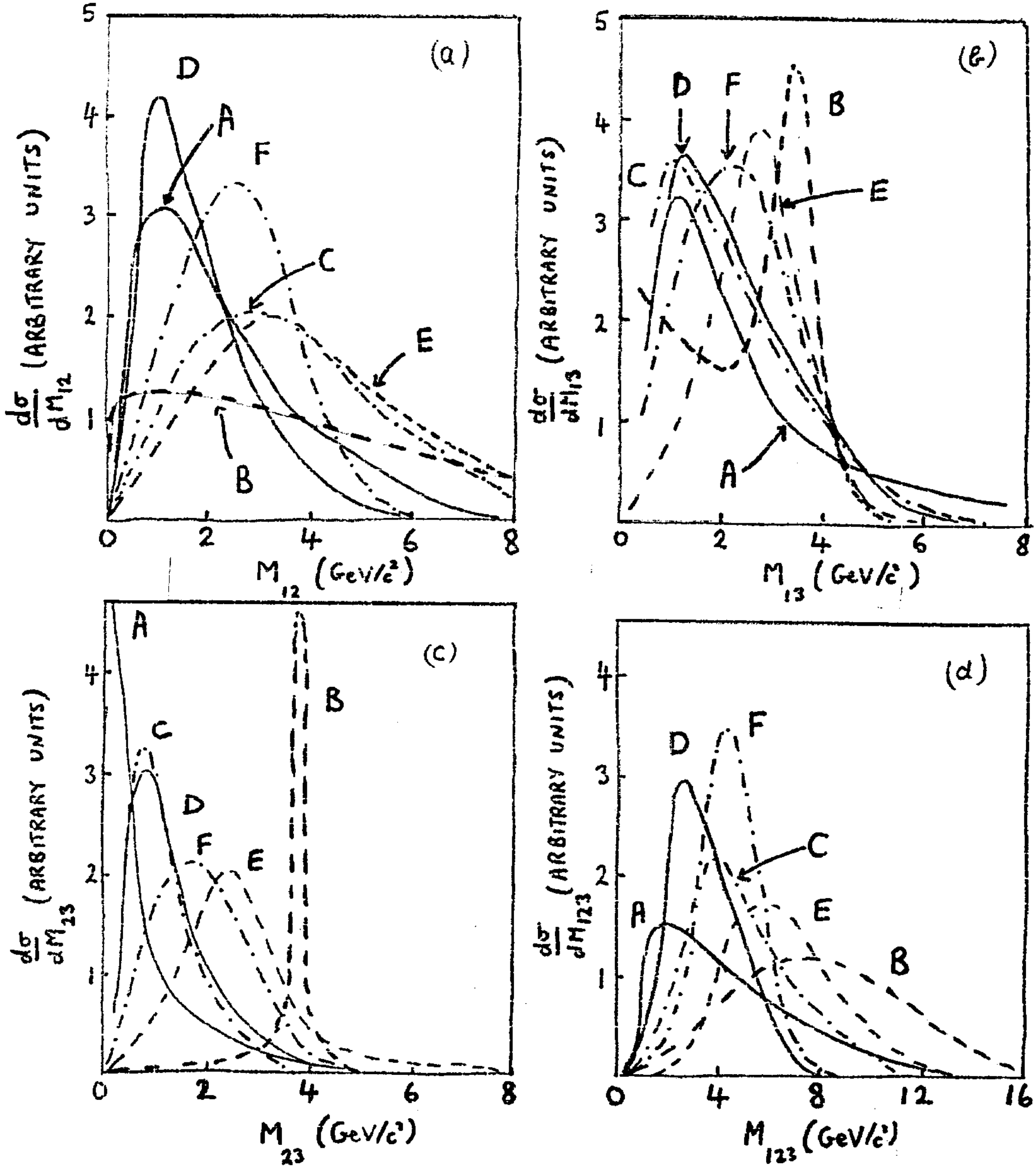
(a)
D
A
F
C
E
B
$\frac{d\sigma}{dM_{12}}$ (ARBITRARY UNITS)
M_{12} (GeV/c²)
(b)
D
F
B
C
E
A
$\frac{d\sigma}{dM_{13}}$ (ARBITRARY UNITS)
M_{13} (GeV/c²)
(c)
A
C
D
F
E
B
$\frac{d\sigma}{dM_{23}}$ (ARBITRARY UNITS)
M_{23} (GeV/c²)
(d)
D
F
C
A
E
B
$\frac{d\sigma}{dM_{123}}$ (ARBITRARY UNITS)
M_{123} (GeV/c²)

Fig.13

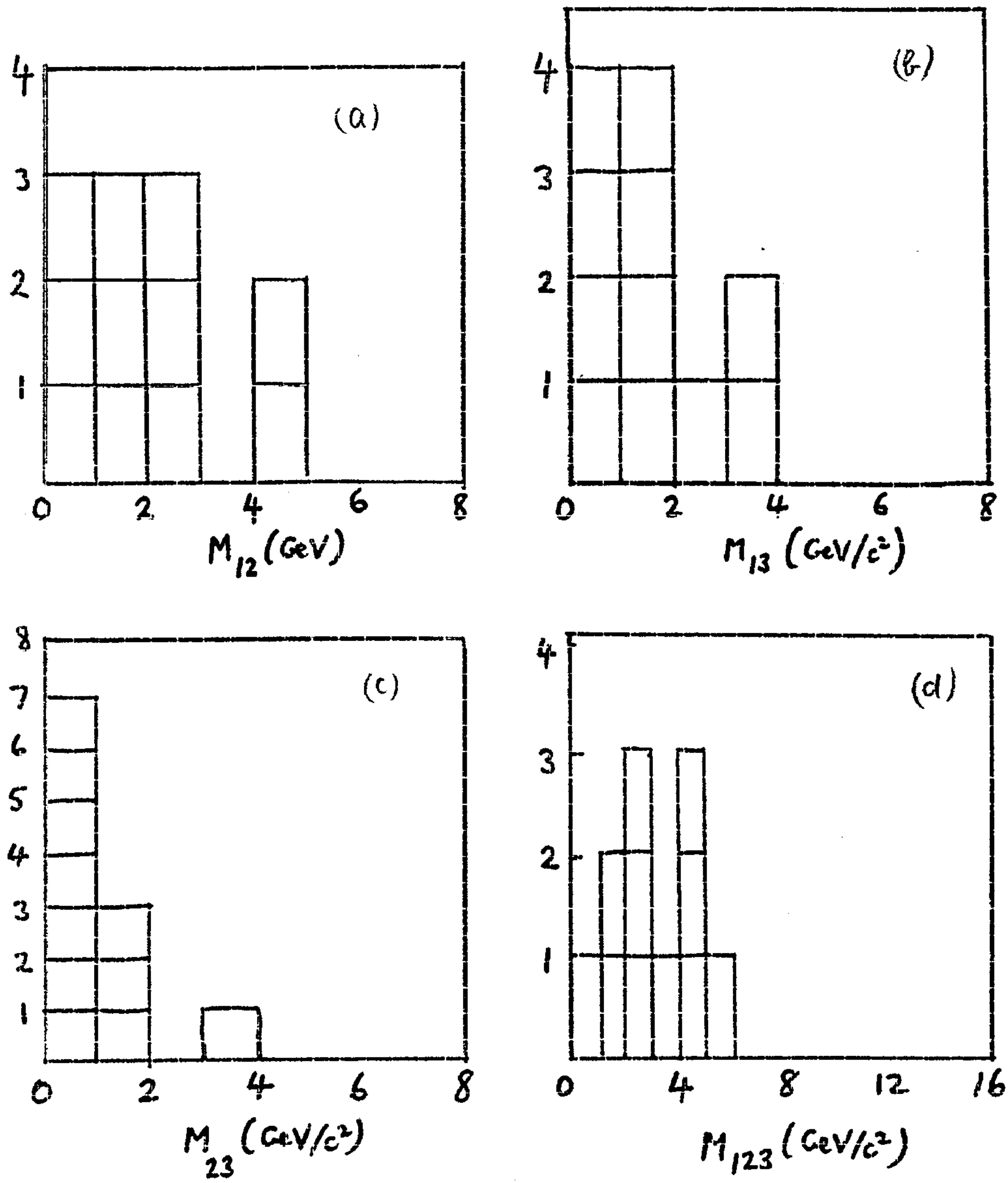

Fig. 14

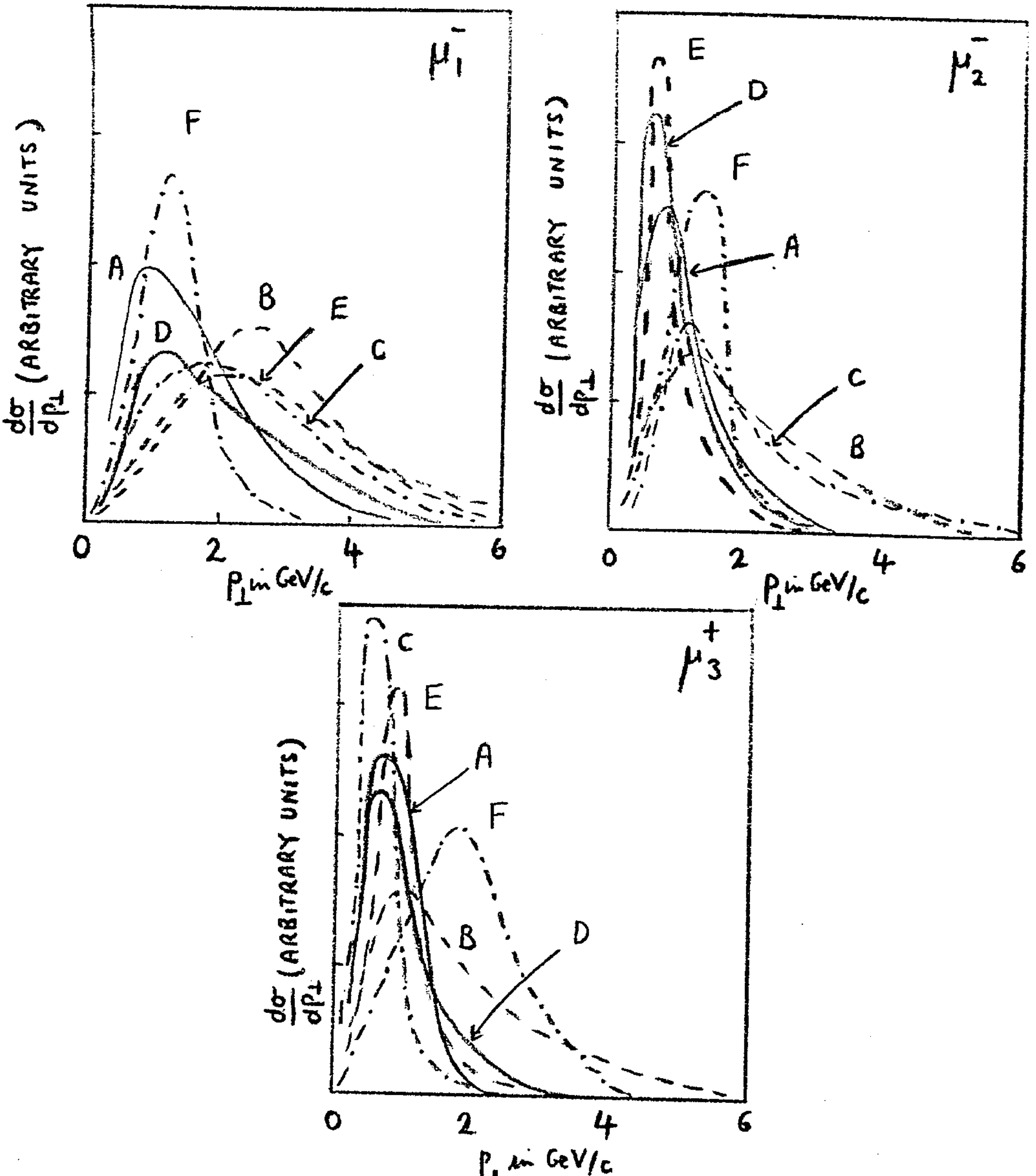

μ₁⁻
F
A
B
E
D
C
dσ/dp⊥ (ARBITRARY UNITS)
0
2
4
6
P⊥ in GeV/c
μ₂⁻
E
D
F
A
C
B
dσ/dp⊥ (ARBITRARY UNITS)
0
2
4
6
P⊥ in GeV/c
μ₃⁺
C
E
A
F
B
D
dσ/dp⊥ (ARBITRARY UNITS)
0
2
4
6
P⊥ in GeV/c

Fig.15

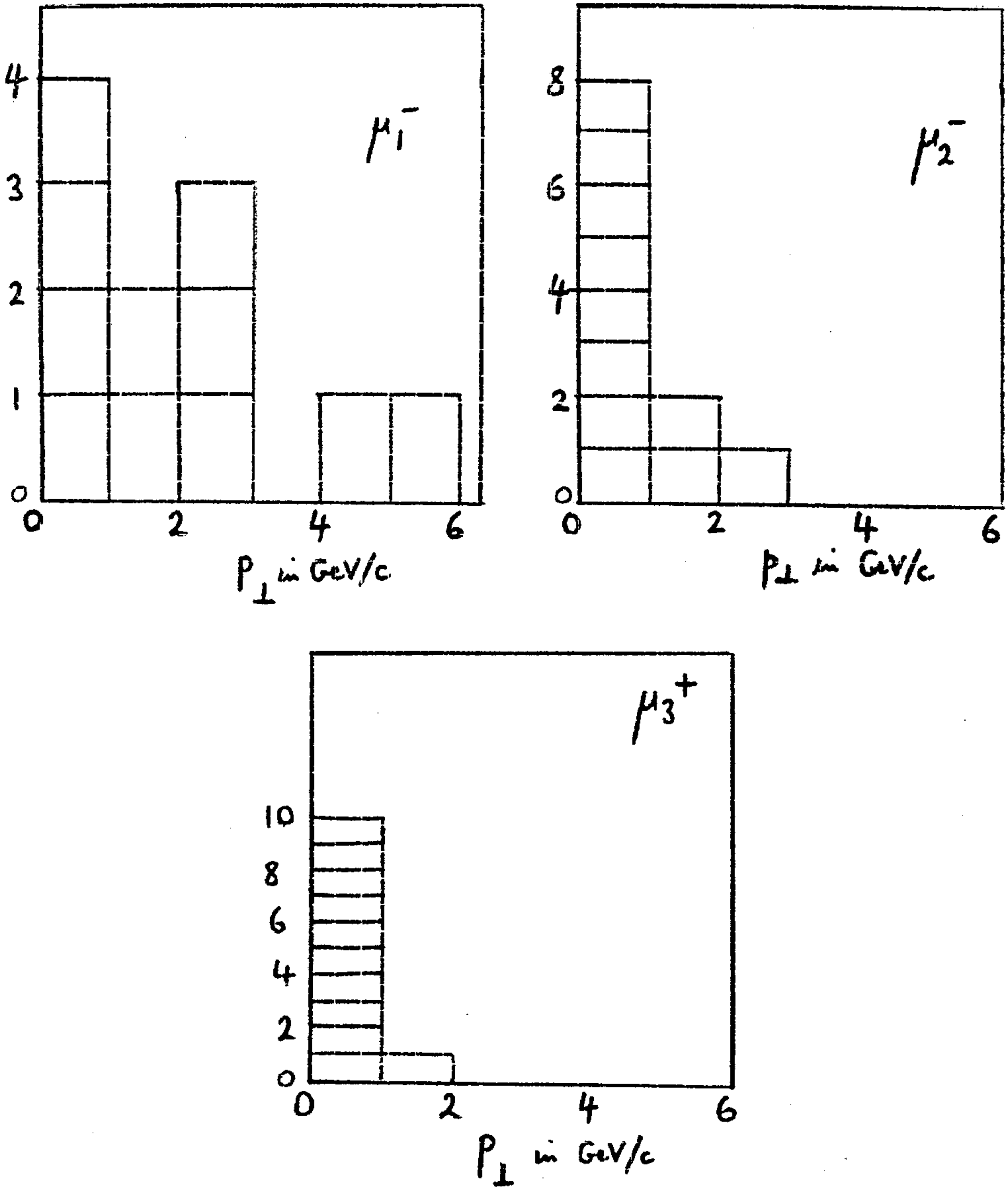

Fig.16

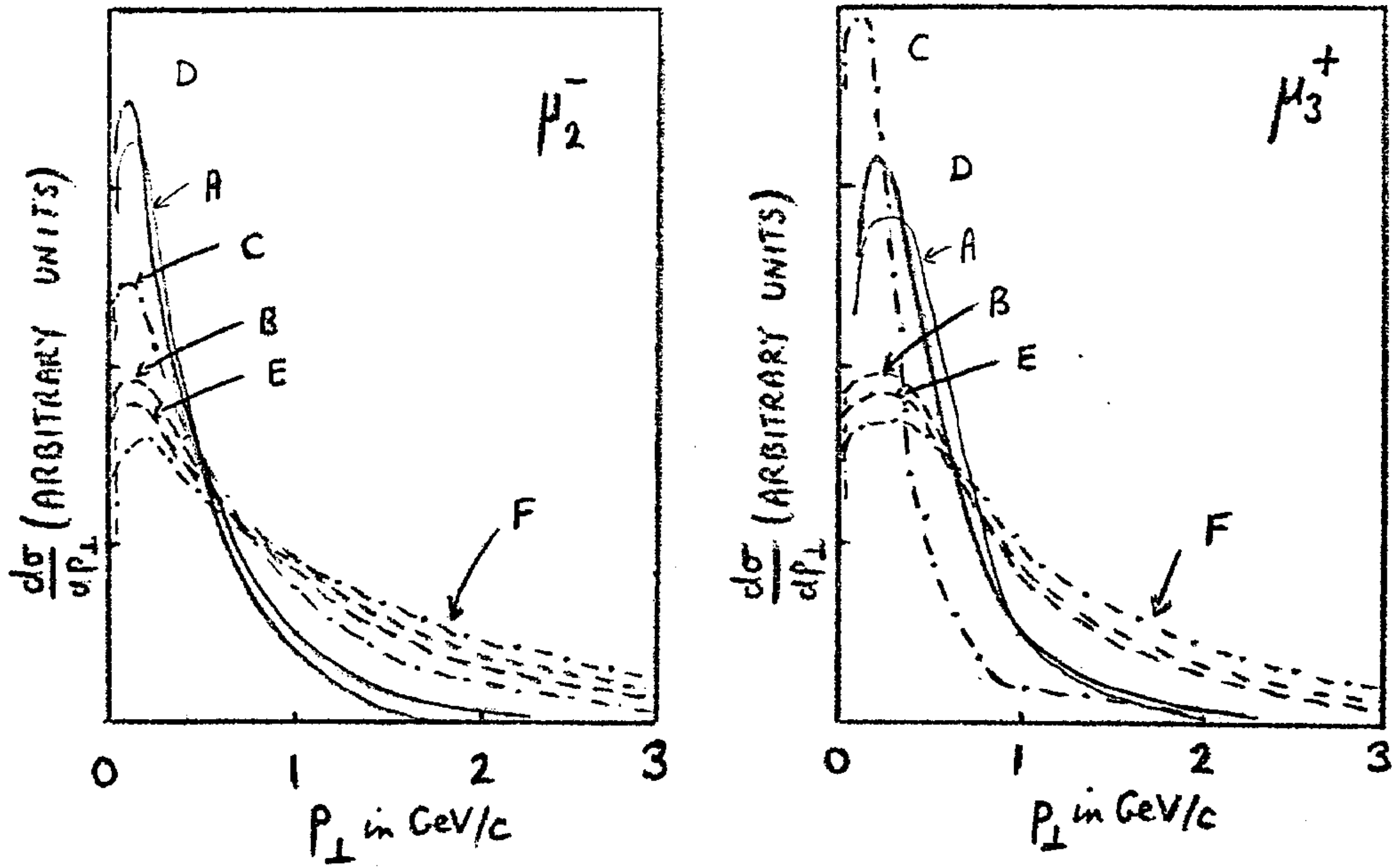

D
A
C
B
E
F
μ_2^-
$\frac{d\sigma}{dp_\perp}$ (ARBITRARY UNITS)
0
1
2
3
$p_\perp$ in GeV/c
C
D
A
B
E
F
μ_3^+
$\frac{d\sigma}{dp_\perp}$ (ARBITRARY UNITS)
0
1
2
3
$p_\perp$ in GeV/c

Fig.17

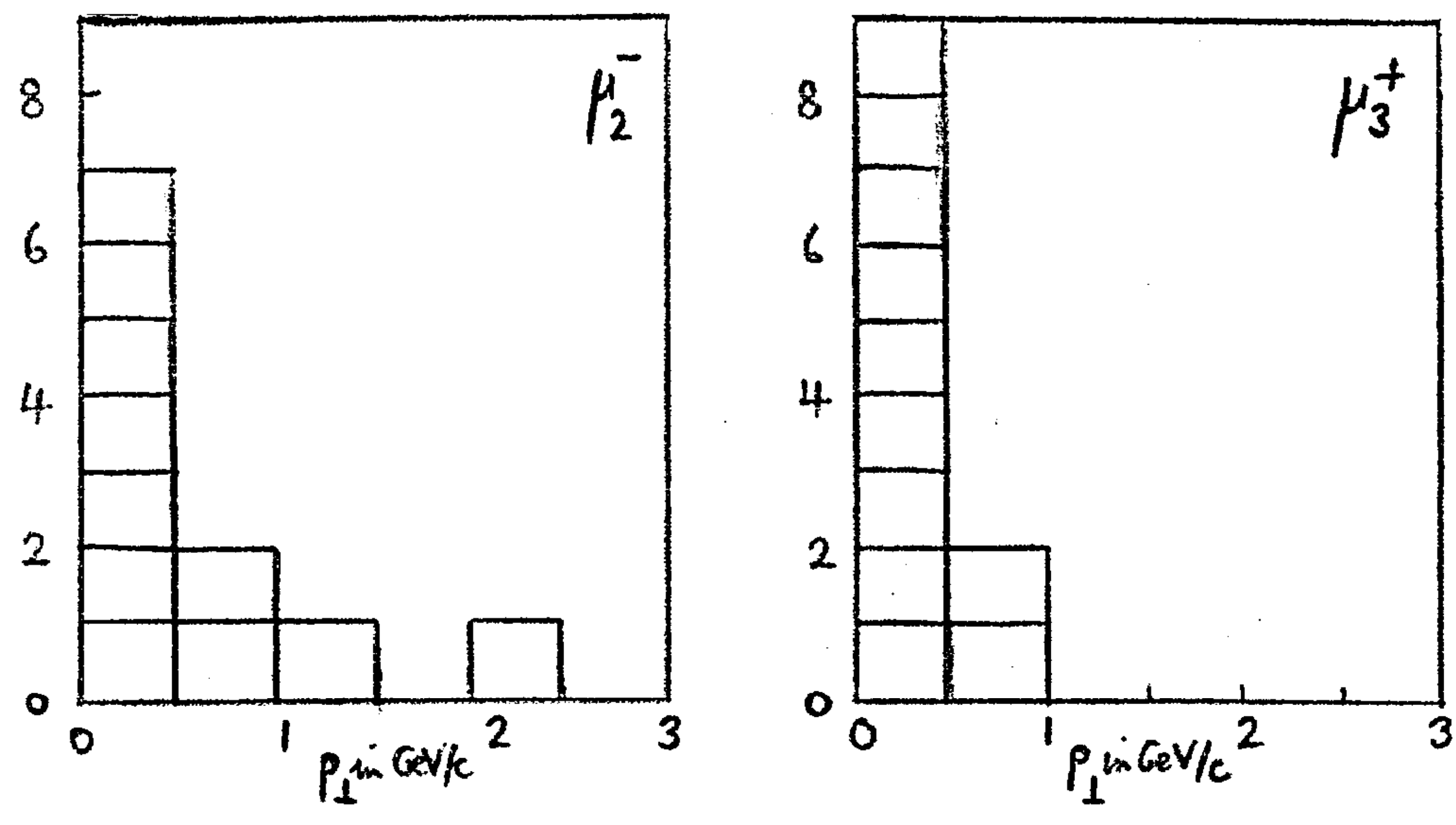

μ_2^-
8
6
4
2
0
0
1
2
3
$p_\perp$ in GeV/c
μ_3^+
8
6
4
2
0
0
1
2
3
$p_\perp$ in GeV/c

Fig. 18

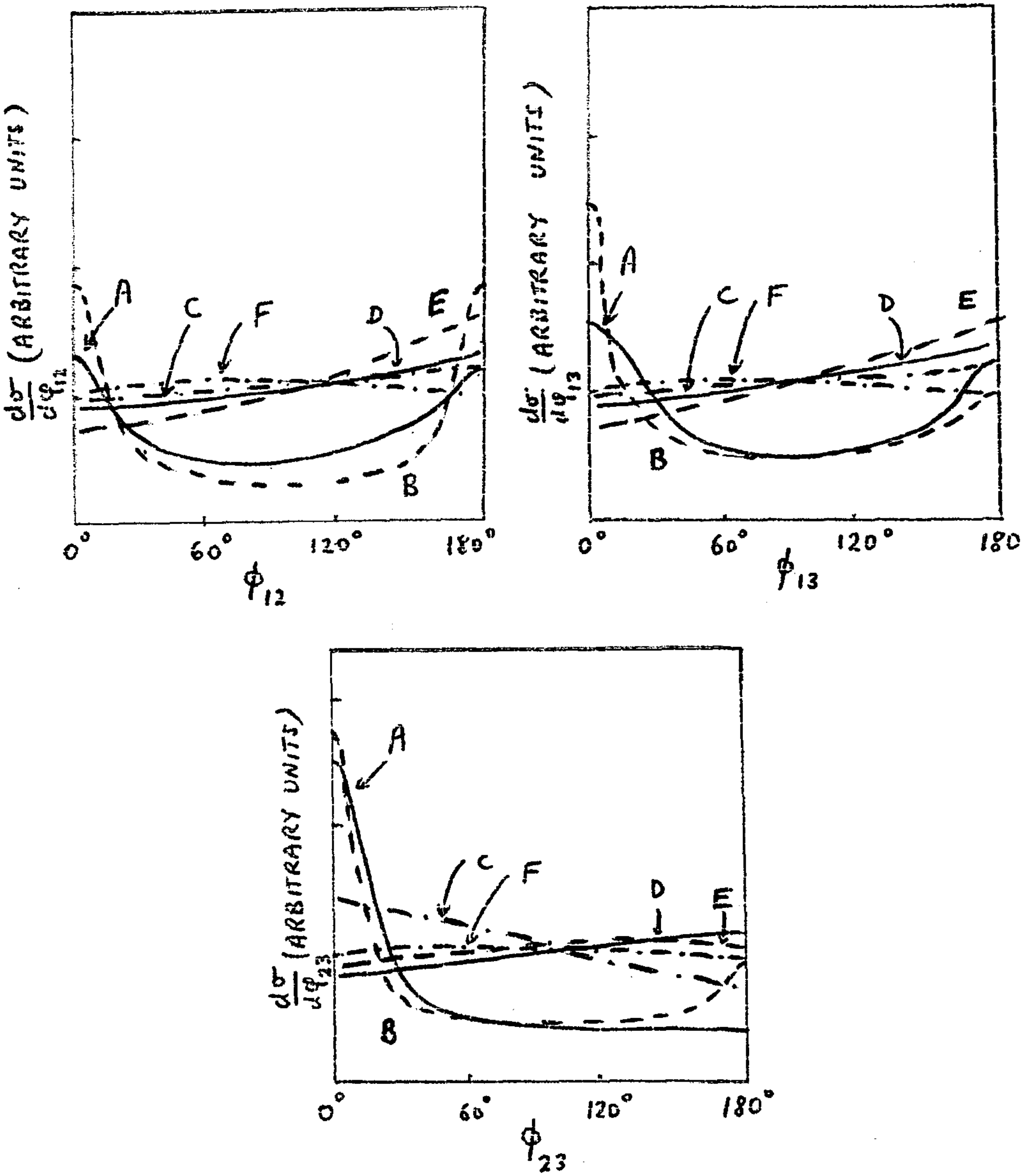

A
C
F
D
E
B
0°
60°
120°
180°
ϕ_{12}
$\frac{d\sigma}{d\varphi_{12}}$ (ARBITRARY UNITS)
A
C
F
D
E
B
0°
60°
120°
180
ϕ_{13}
$\frac{d\sigma}{d\varphi_{13}}$ (ARBITRARY UNITS)
A
C
F
D
E
B
0°
60°
120°
180°
ϕ_{23}
$\frac{d\sigma}{d\varphi_{23}}$ (ARBITRARY UNITS)

Fig. 19

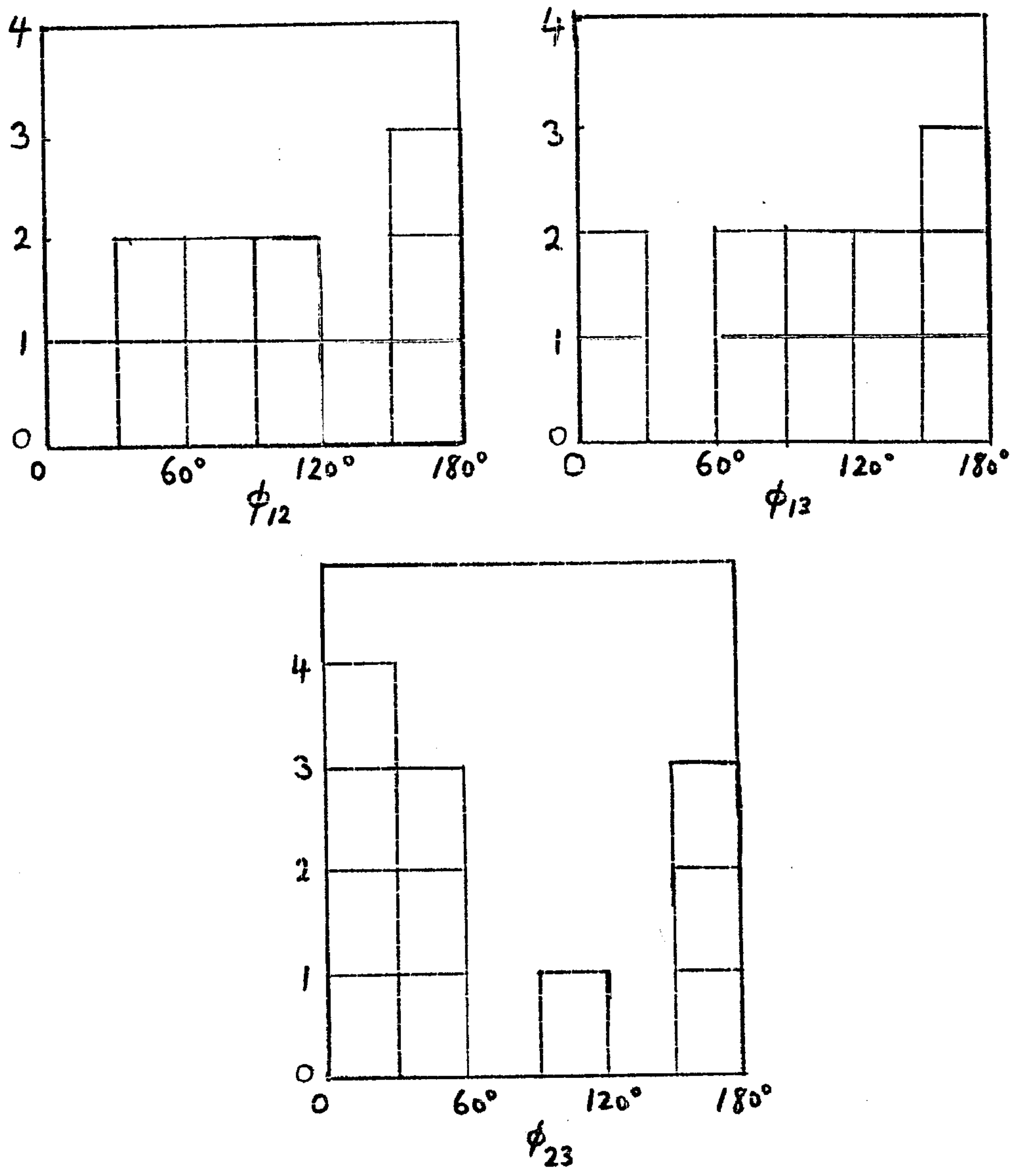

4
3
2
1
0
0
60°
120°
180°
ϕ_{12}
4
3
2
1
0
0
60°
120°
180°
ϕ_{13}
4
3
2
1
0
0
60°
120°
180°
ϕ_{23}

Fig. 20

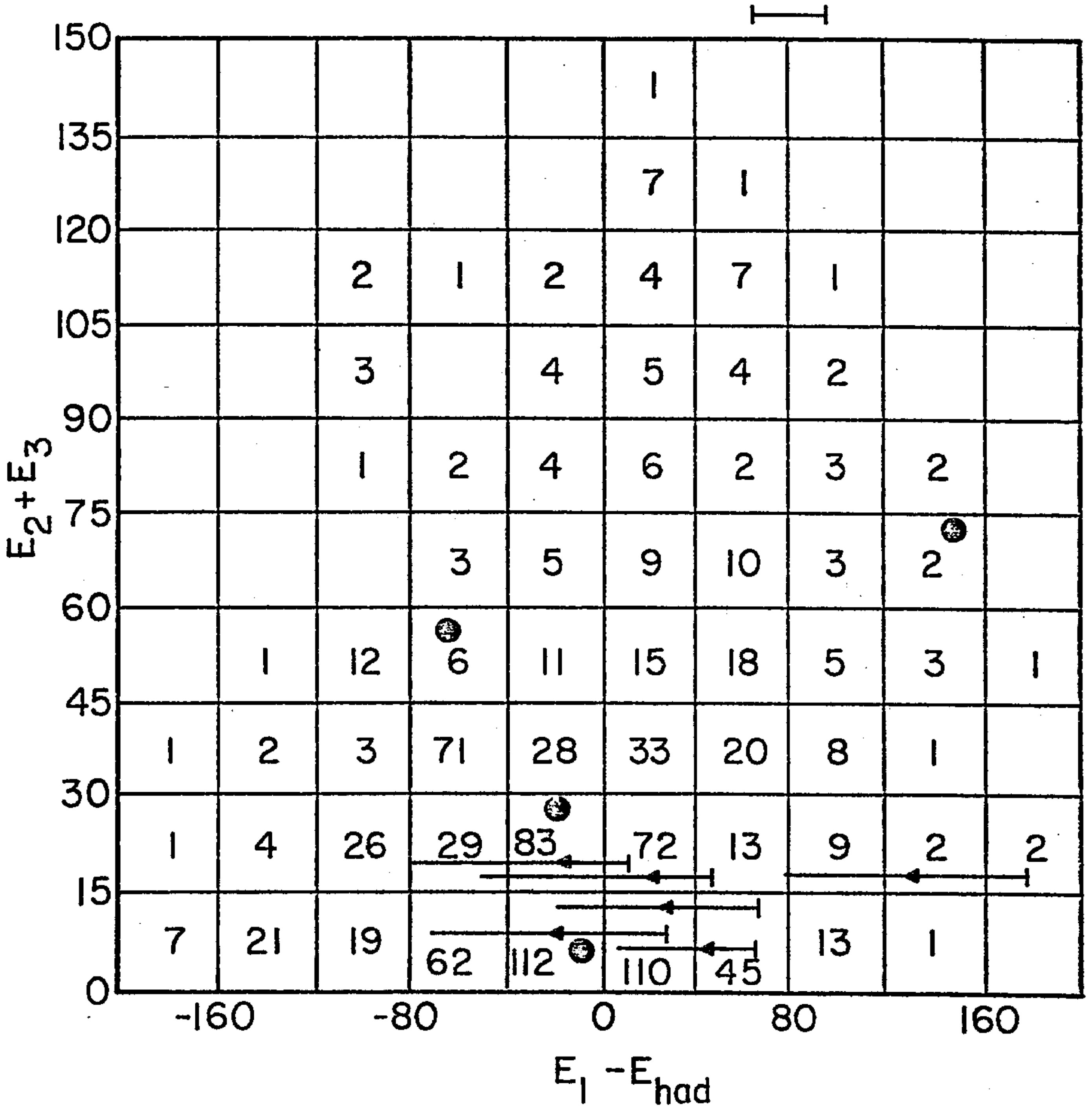

150
135
120
105
90
75
60
45
30
15
0
-160
-80
0
80
160
E_2+E_3
E_1-E_{had}
1
7 1
2 1 2 4 7 1
3 4 5 4 2
1 2 4 6 2 3 2
3 5 9 10 3 2
1 12 6 11 15 18 5 3 1
1 2 3 71 28 33 20 8 1
1 4 26 29 83 72 13 9 2 2
7 21 19 62 112 110 45 13 1

Fig. 21

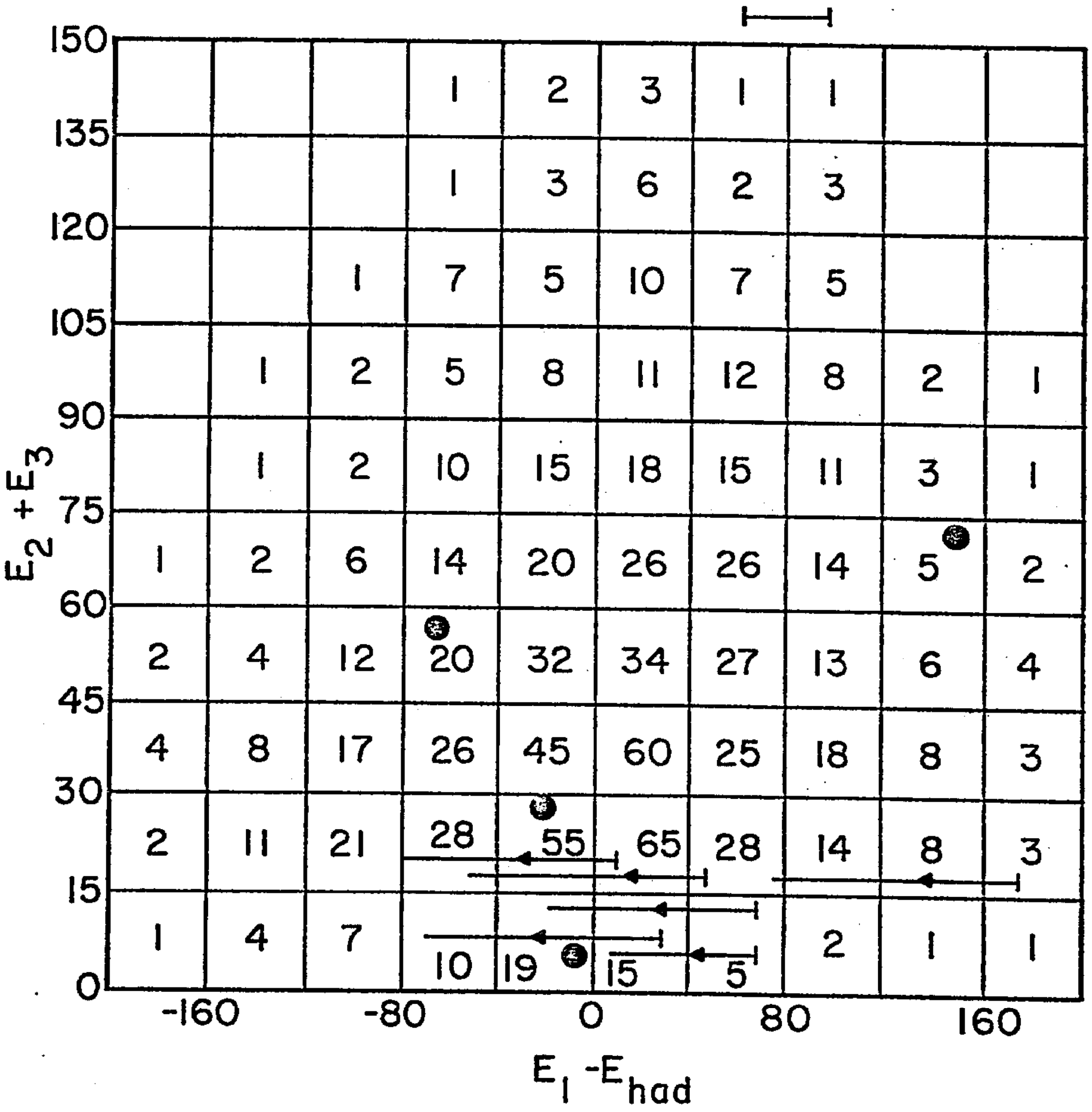

150
135
120
105
90
75
60
45
30
15
0
-160
-80
0
80
160
$E_2 + E_3$
$E_1 - E_{had}$
1 2 3 1 1
1 3 6 2 3
1 7 5 10 7 5
1 2 5 8 11 12 8 2 1
1 2 10 15 18 15 11 3 1
1 2 6 14 20 26 26 14 5 2
2 4 12 20 32 34 27 13 6 4
4 8 17 26 45 60 25 18 8 3
2 11 21 28 55 65 28 14 8 3
1 4 7 10 19 15 5 2 1 1

Fig.22

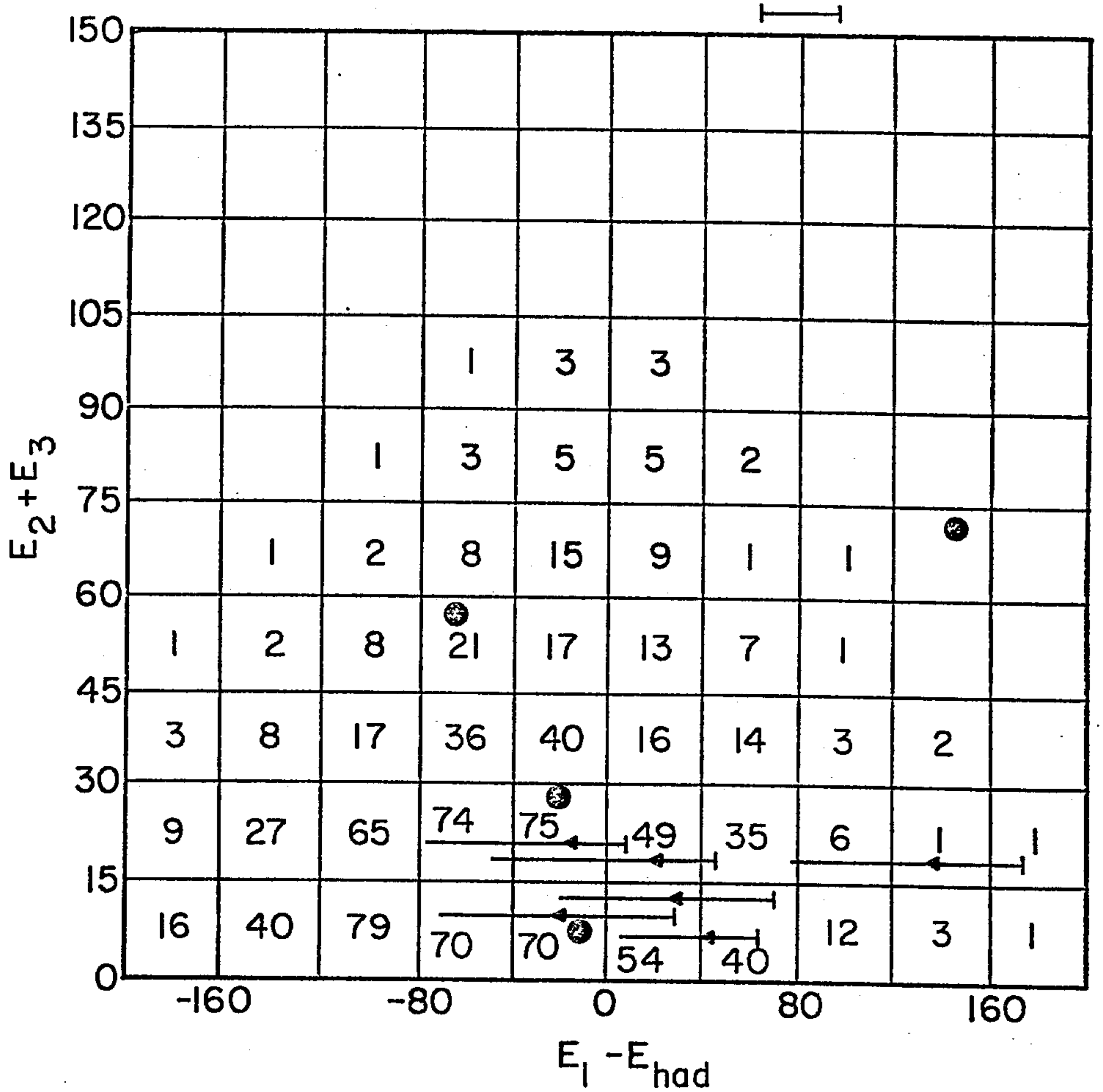

150
135
120
105
90
75
60
45
30
15
0
-160
-80
0
80
160
E_2+E_3
E_1-E_{had}
1 3 3
1 3 5 5 2
1 2 8 15 9 1 1
1 2 8 21 17 13 7 1
3 8 17 36 40 16 14 3 2
9 27 65 74 75 49 35 6 1 1
16 40 79 70 70 54 40 12 3 1

Fig.23

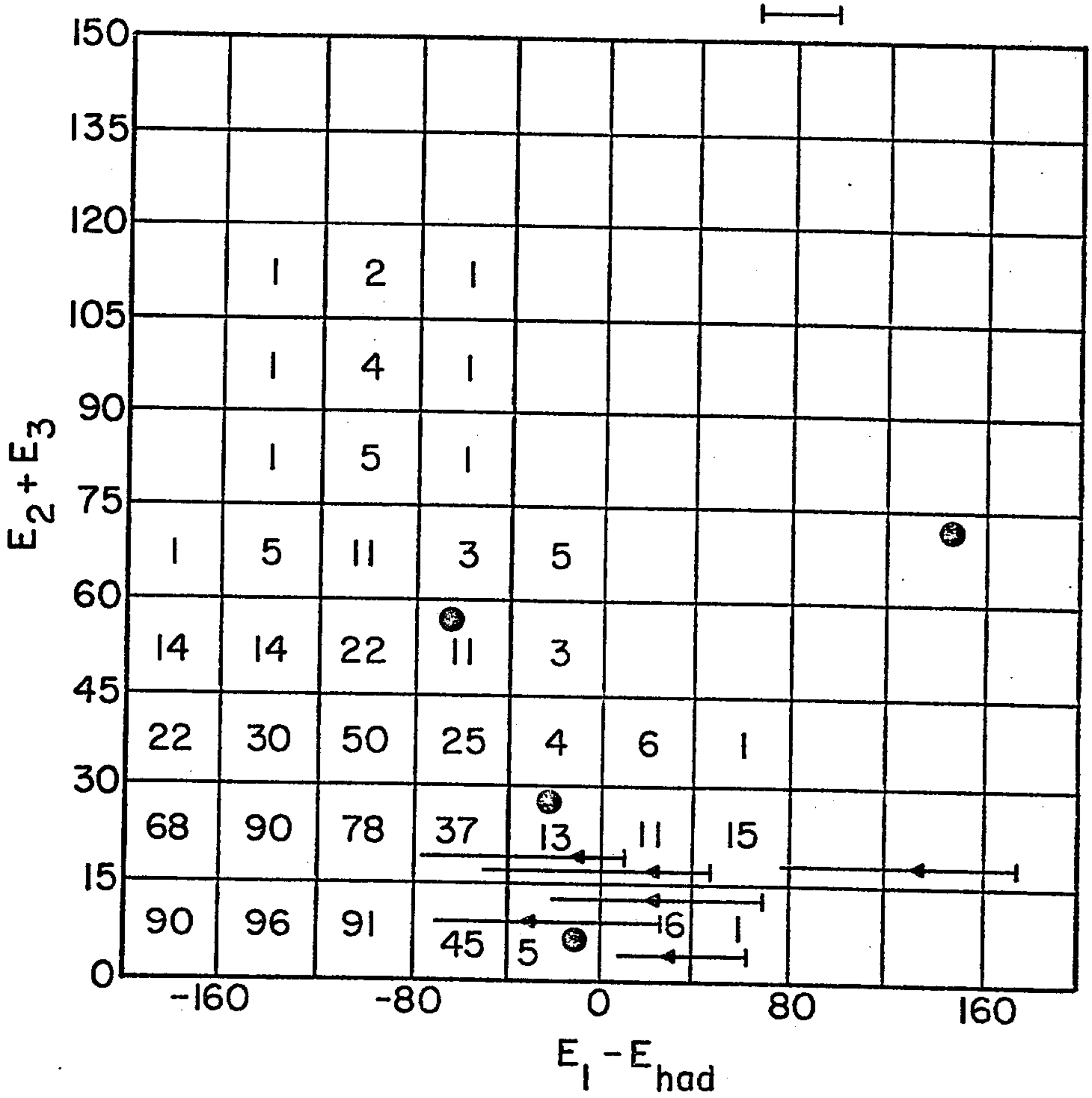
150
135
120
105
90
75
60
45
30
15
0
-160
-80
0
80
160
E_2+E_3
E_1-E_{had}
1 2 1
1 4 1
1 5 1
1 5 11 3 5
14 14 22 11 3
22 30 50 25 4 6 1
68 90 78 37 13 11 15
90 96 91 45 5 16 1

Fig. 24

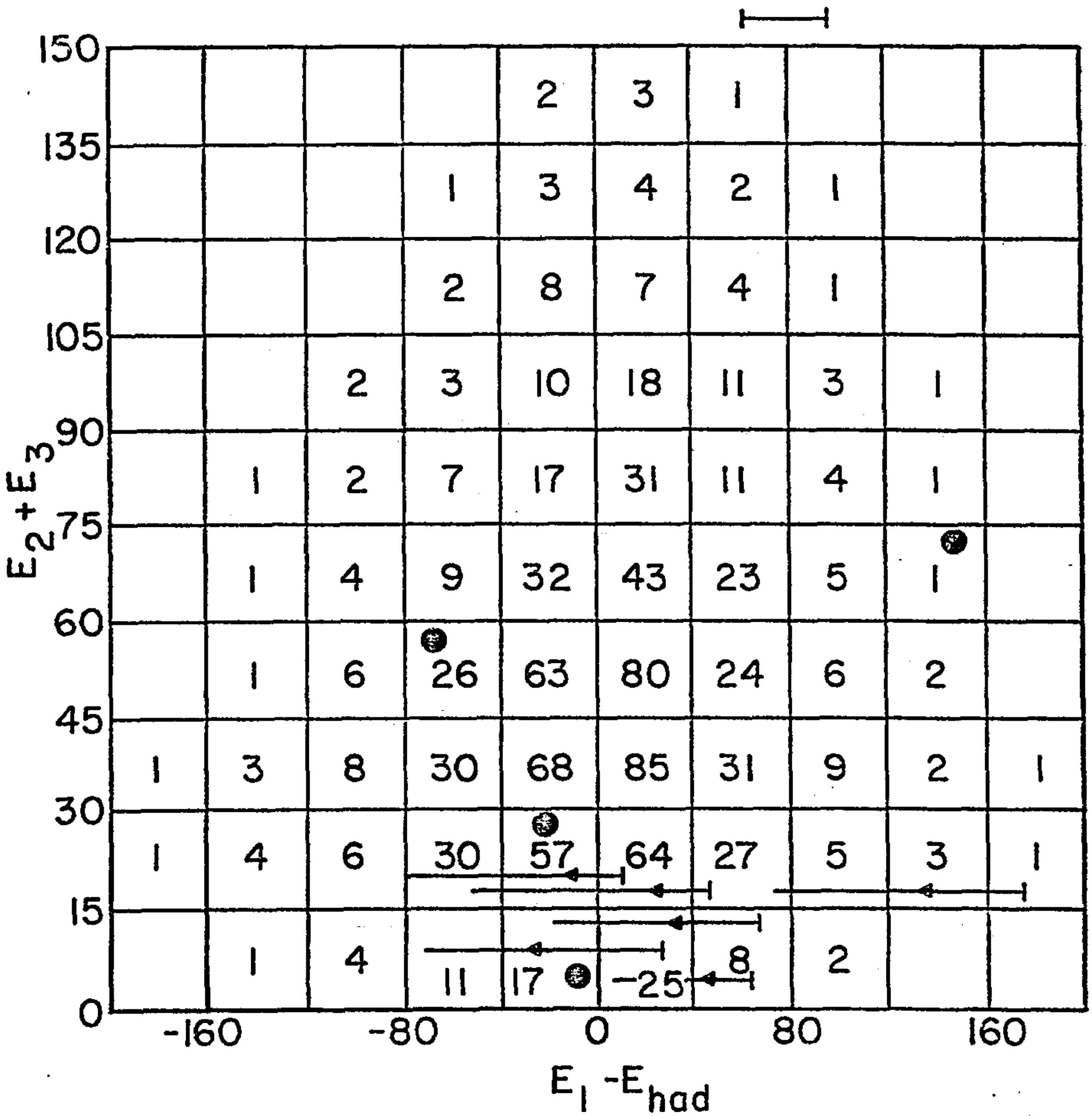

150
135
120
105
90
75
60
45
30
15
0
-160
-80
0
80
160
E_2+E_3
$E_1 - E_{had}$
2 3 1
1 3 4 2 1
2 8 7 4 1
2 3 10 18 11 3 1
1 2 7 17 31 11 4 1
1 4 9 32 43 23 5 1
1 6 26 63 80 24 6 2
1 3 8 30 68 85 31 9 2 1
1 4 6 30 57 64 27 5 3 1
1 4 11 17 -25 8 2

Fig.25

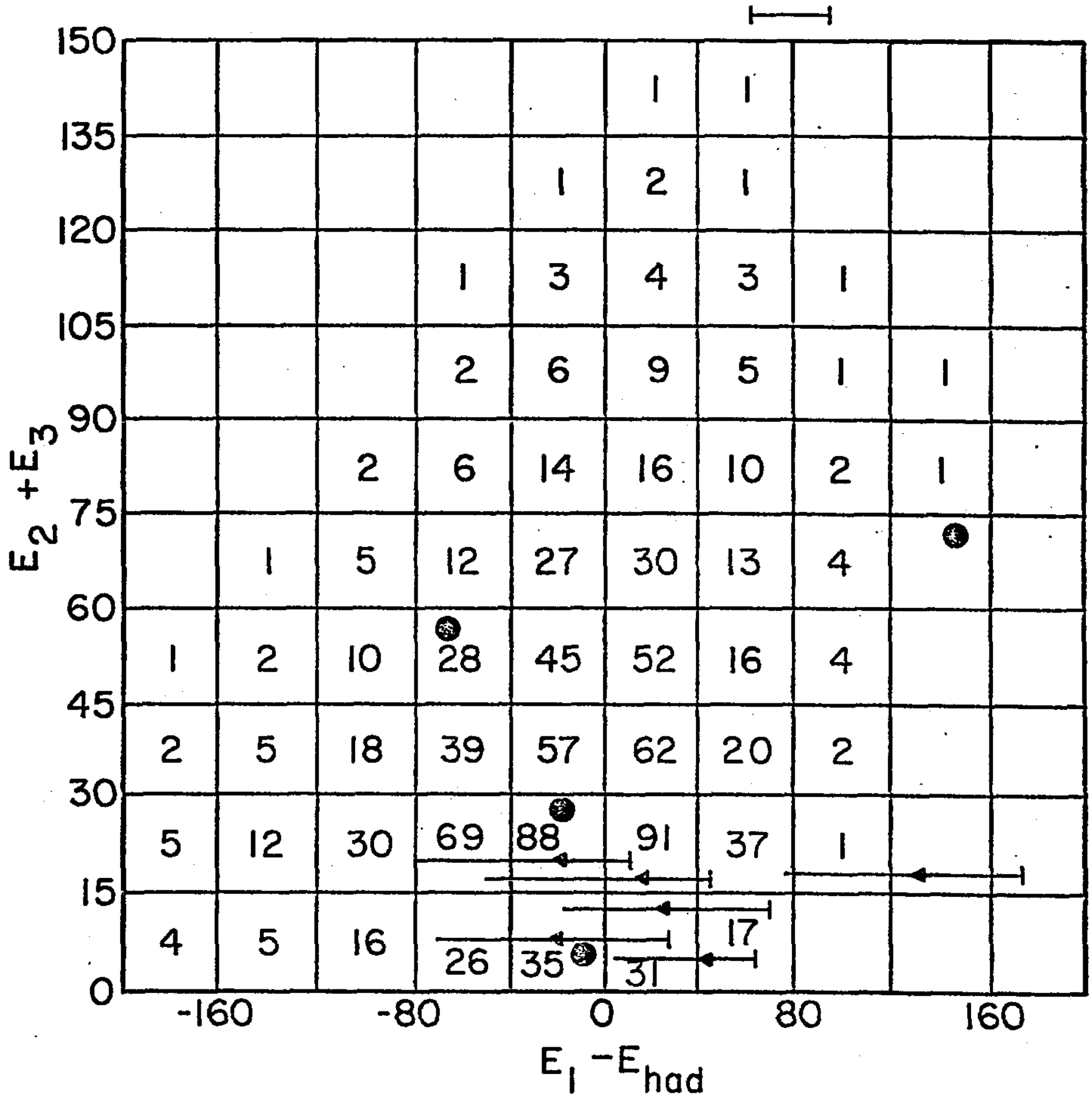

Fig. 26

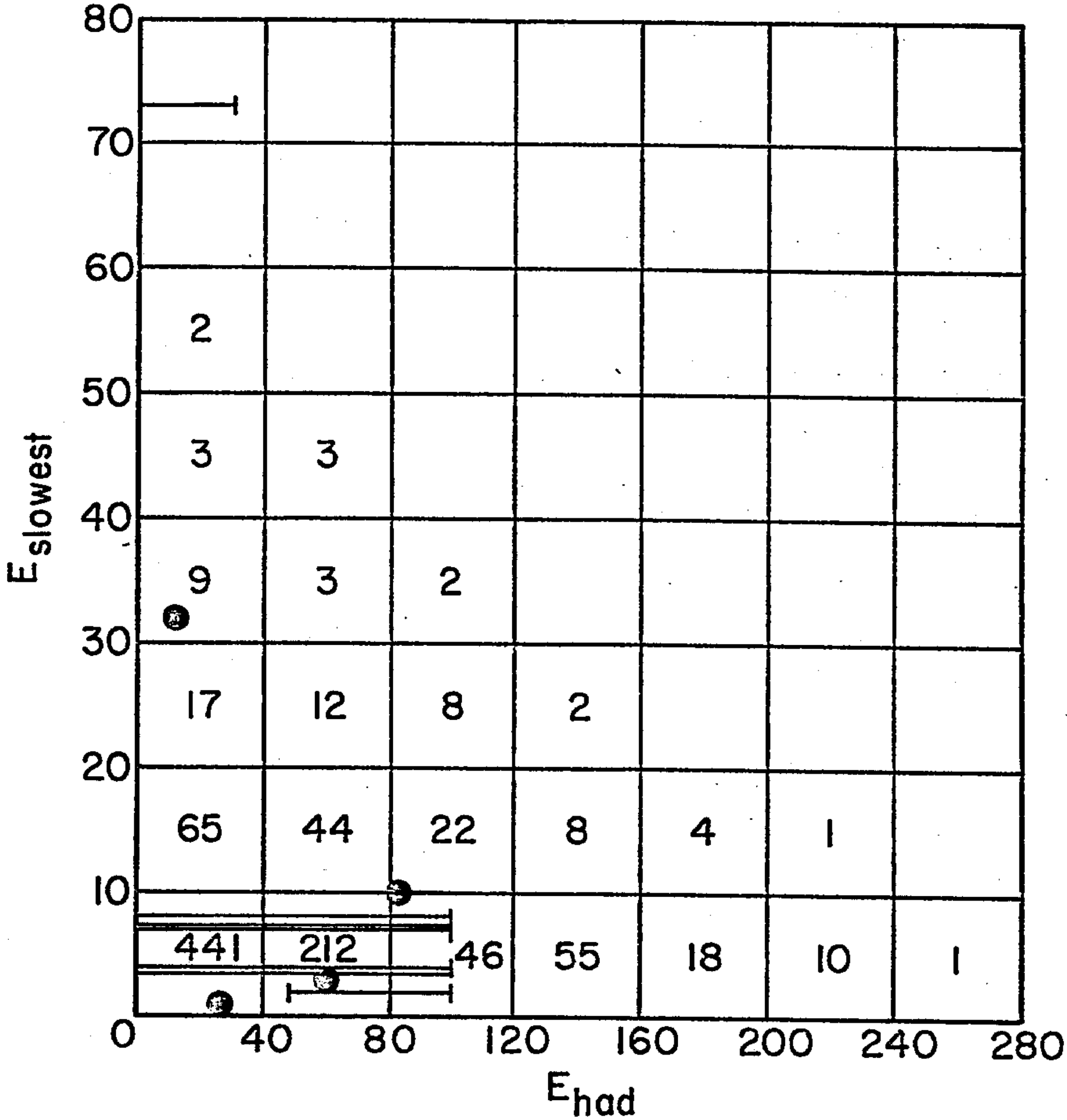

80
70
60
50
40
30
20
10
0
40
80
120
160
200
240
280
E slowest
E had
2
3
3
9
3
2
17
12
8
2
65
44
22
8
4
1
441
212
46
55
18
10
1

Fig.27

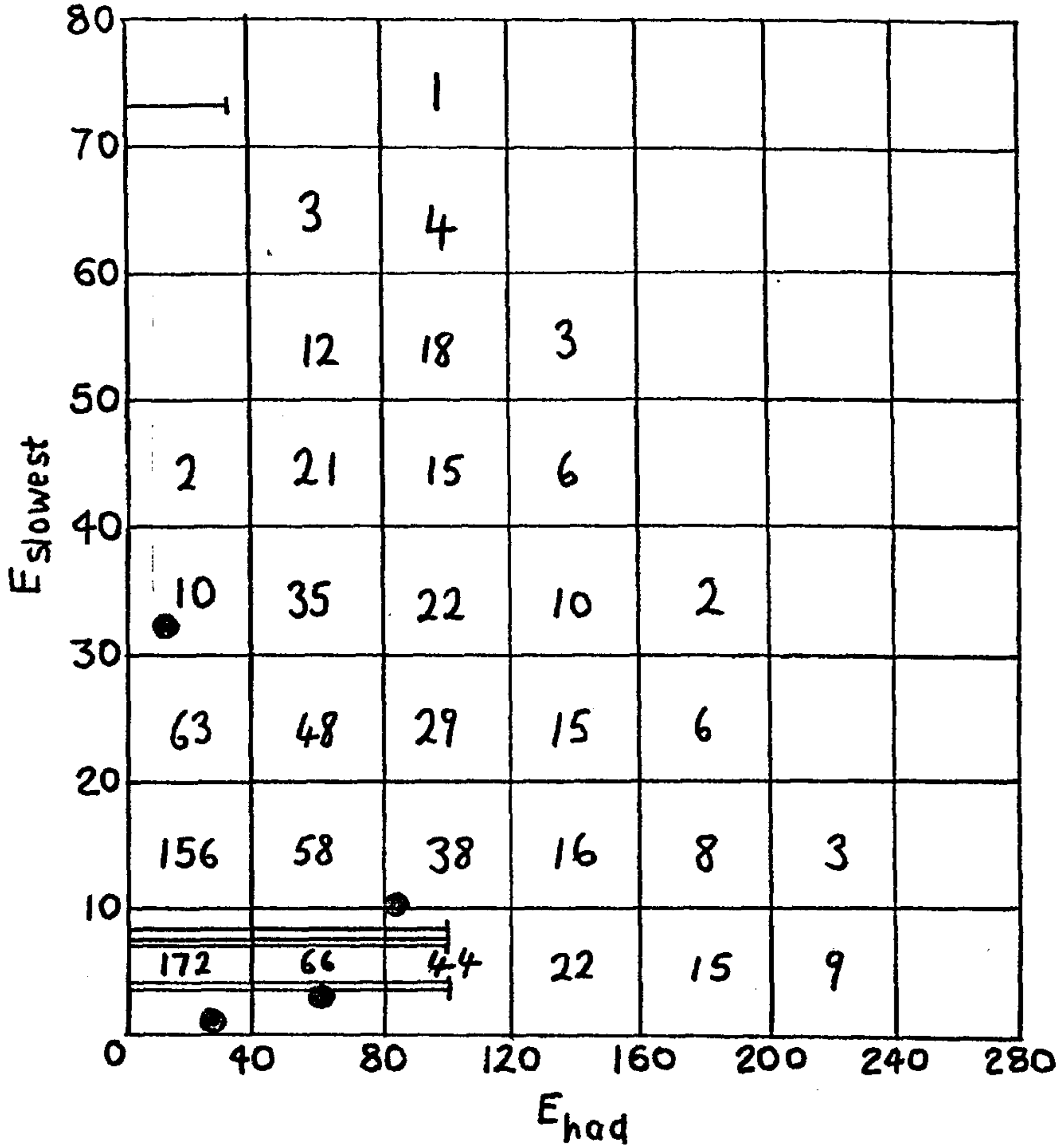

80
70
60
50
40
30
20
10
0
40
80
120
160
200
240
280
$E_{slowest}$
E_{had}
1
3
4
12
18
3
2
21
15
6
10
35
22
10
2
63
48
29
15
6
156
58
38
16
8
3
172
66
44
22
15
9

Fig. 28

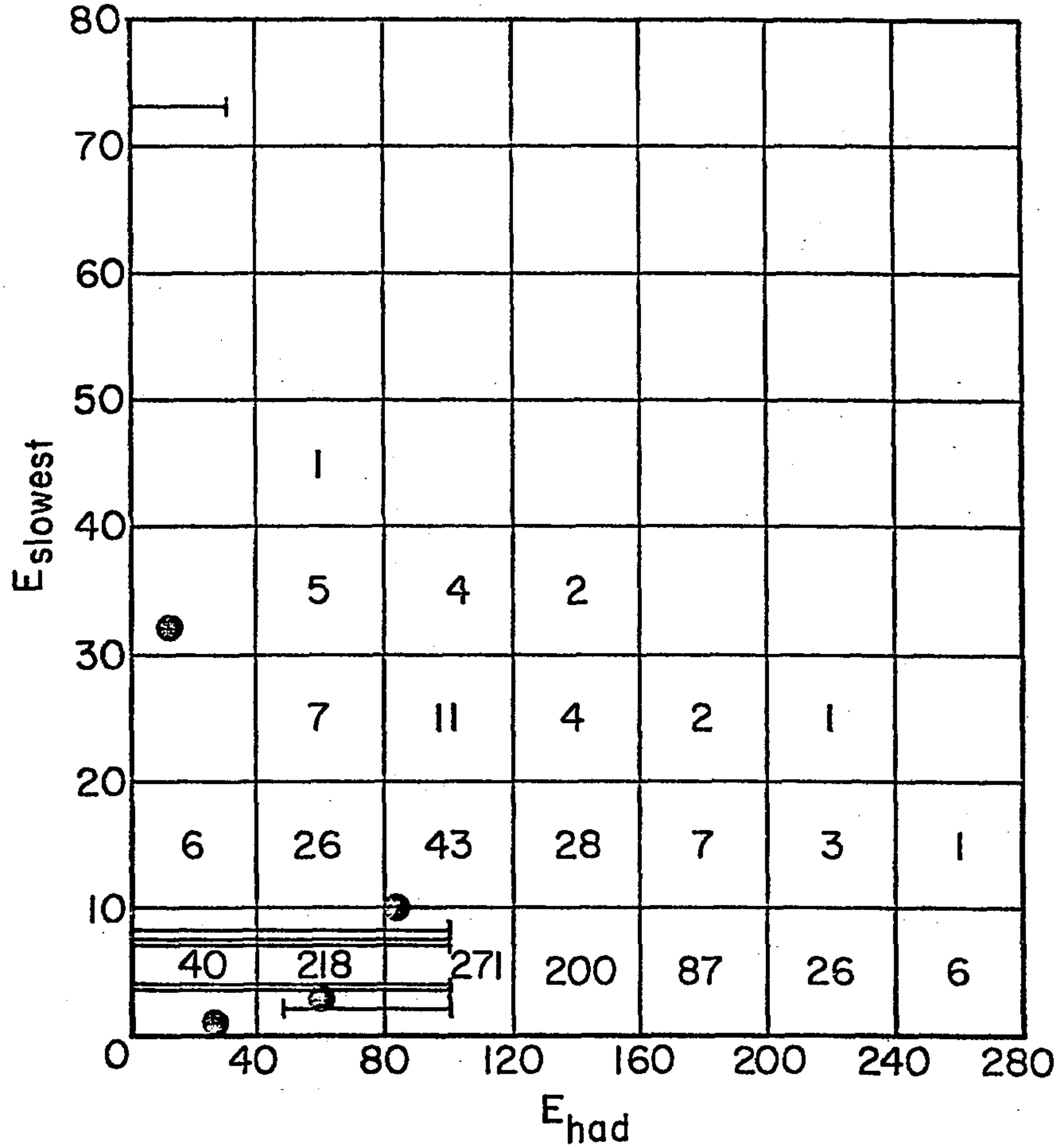

E_slowest
E_had
0
10
20
30
40
50
60
70
80
40
80
120
160
200
240
280
1
5
4
2
7
11
4
2
1
6
26
43
28
7
3
1
40
218
271
200
87
26
6

Fig. 29

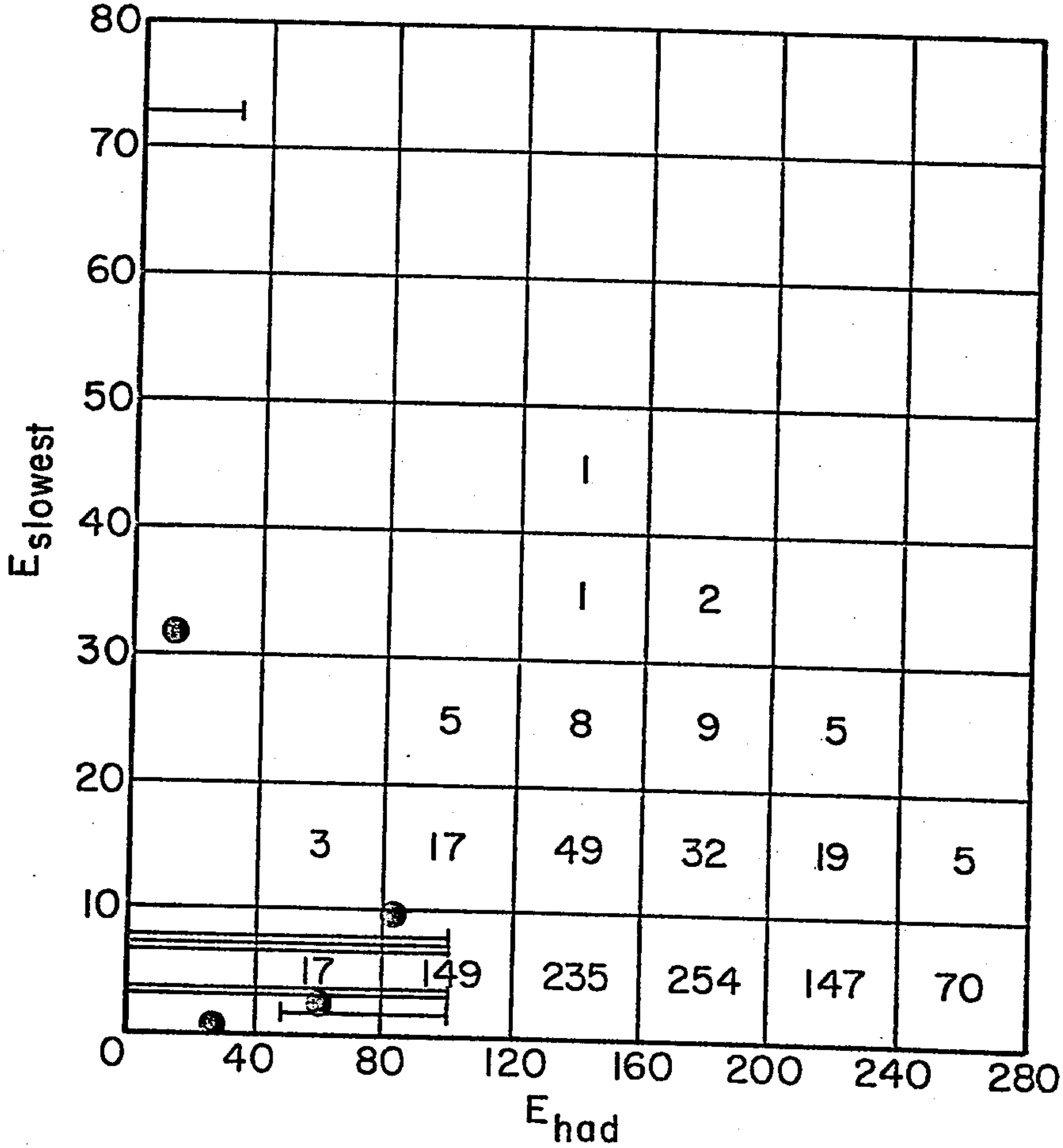

80
70
60
50
40
30
20
10
0
$E_{slowest}$
1
1
2
5
8
9
5
3
17
49
32
19
5
17
149
235
254
147
70
40
80
120
160
200
240
280
E_{had}

Fig. 30

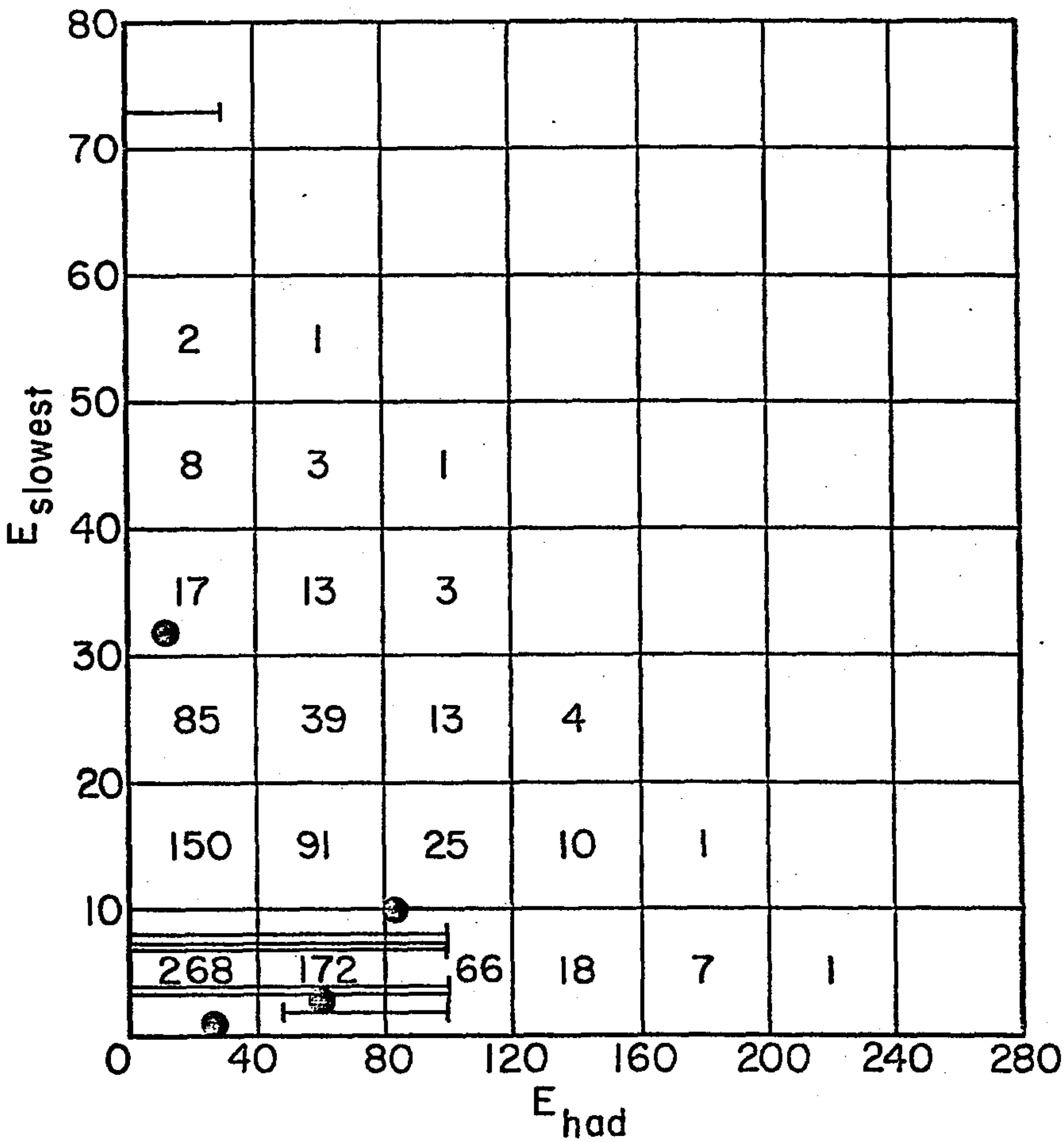

80
70
60
50
40
30
20
10
0
40
80
120
160
200
240
280
$E_{slowest}$
E_{had}
2
1
8
3
1
17
13
3
85
39
13
4
150
91
25
10
1
268
172
66
18
7
1

Fig. 31

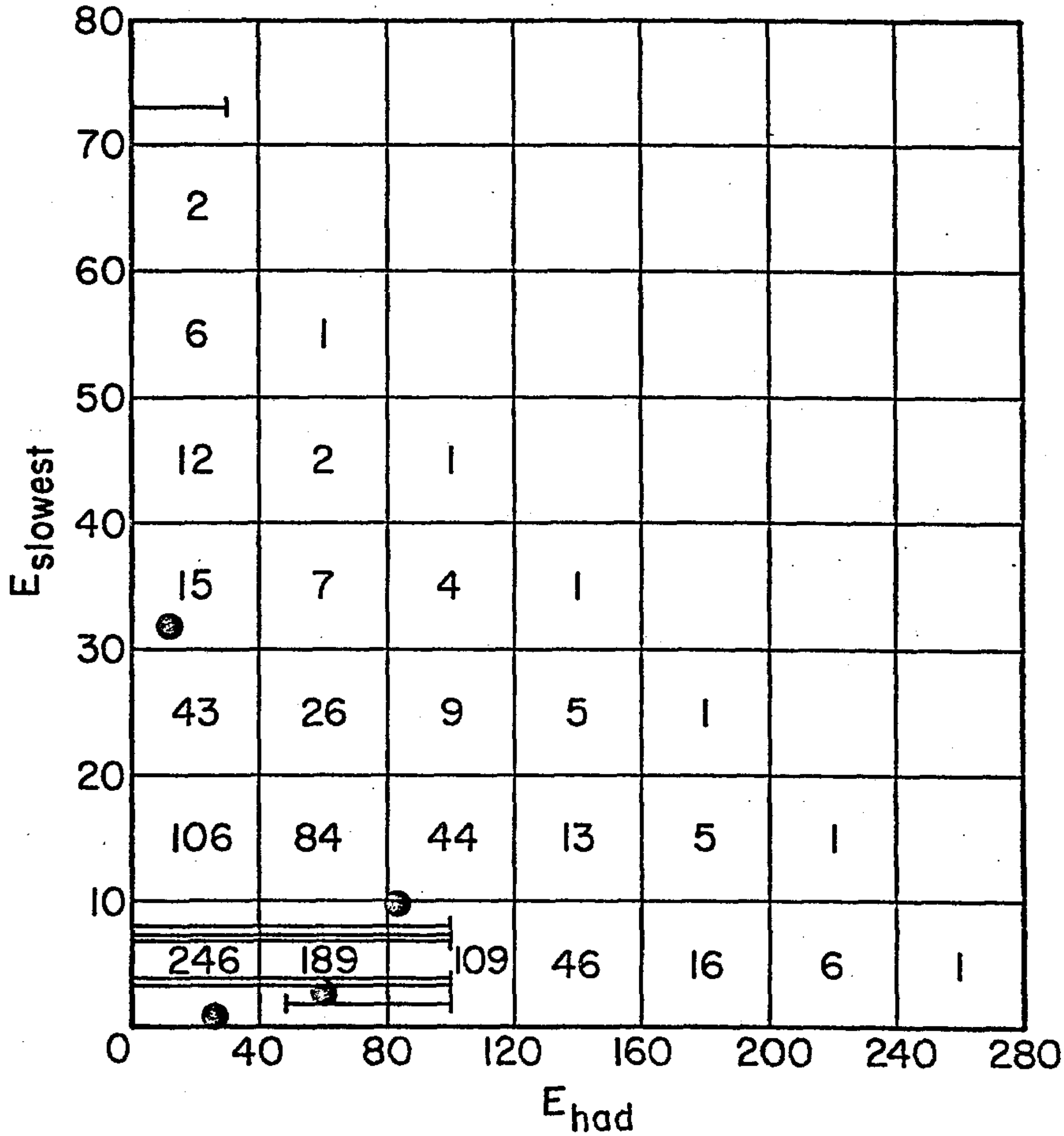
80
70
60
50
40
30
20
10
0
40
80
120
160
200
240
280
Eslowest
Ehad
2
6
1
12
2
1
15
7
4
1
43
26
9
5
1
106
84
44
13
5
1
246
189
109
46
16
6
1